IEEE Access
Multidisciplinary | Rapid Review | Open Access Journal

Received May 30, 2017, accepted July 13, 2017, date of publication July 27, 2017, date of current version August 14, 2017.

Digital Object Identifier 10.1109/ACCESS.2017.2732498

Analysis of Load Balancing and Interference Management in Heterogeneous Cellular Networks

ZIAUL HAQ ABBAS[1], FAZAL MUHAMMAD[2], (Student Member, IEEE), AND LEI JIAO[3], (Member, IEEE)

[1]Faculty of Electrical Engineering, Ghulam Ishaq Khan Institute of Engineering Sciences and Technology, Topi 23640, Pakistan
[2]Faculty of Electrical Engineering, City University of Science and Information Technology, Peshawar 25000, Pakistan
[3]Department of Information and Communication Technology, University of Agder (UiA), N-4898 Grimstad, Norway

Corresponding author: Fazal Muhammad (fazal.muhammad@cusit.edu.pk)

ABSTRACT To meet the current cellular capacity demands, proactive offloading is required in heterogeneous cellular networks (HetCNets) comprising of different tiers of base stations (BSs), e.g., small-cell BSs (sBSs) and conventional macro-cell BSs (mBSs). Each tier differs from the others in terms of BS transmit power, spatial density, and association bias. Consequently, the coverage range of each tier BSs is also different from others. Due to low transmit power, a fewer number of users are associated to an sBS as compared with mBS. Thus, inefficient utilization of small-cell resources occurs. To balance the load across the network, it is necessary to push users to the underloaded small cells from the overloaded macro-cells. In co-channel deployed HetCNets, mBSs cause heavy inter-cell interference (ICI) to the offloaded users, which significantly affects the network performance gain. To address this issue, we develop a tractable analytical network model abating ICI using reverse frequency allocation (RFA) scheme along with cell range expansion-based user association. We probabilistically characterize coverage probability and user rate while considering RFA with and without selective sBS deployment. Our results demonstrate that selective sBS deployment outperforms other deployment methods.

INDEX TERMS Heterogeneous cellular networks, small-cell BSs, reverse frequency allocation, selective sBS deployment, coverage probability, user rate.

I. INTRODUCTION

User association in heterogeneous cellular networks (HetCNets) (e.g., consisting of macro-cell base stations (mBSs) and small-cell BSs (sBSs)) is based on maximum received power scheme [2]–[4], in which a randomly located user receives maximum power from its associated serving BS. Due to higher transmit power an mBS offers greater coverage to the users than low power sBSs. Due to this transmit power disparity most of the active users connect to mBS, which causes the overloading of mBS and underutilization of the sBSs. Consequently, an imbalanced load arrangement takes place between different tiers of BSs.

Several approaches have been adopted so far in the state-of-the-art to balance the load across a HetCNet. Cell range expansion (CRE) [5], [6] based cell association is one of the efficient load balancing schemes used for load management in HetCNets. In this scheme the load is pushed from the overlaid capacity-strained mBS to the underloaded sBSs by adding a positive biasing factor to the sBSs' transmit power. After employing a biasing factor the coverage range of the sBSs increases which provides more biased received power to the users than that of the maximum received power from the mBS. This, as a consequence, decreases the load on the overlaid mBS by offloading a fraction of users to sBSs and thus the resources of sBSs are efficiently utilized. After users' offloading from the mBS to the expanded coverage region of sBSs, the mBS now acts as a strong interferer, due to which the signal-to-interference-plus-noise ratio (SINR) reduces, consequently, degrading HetCNets' performance [7], [8]. However, this interference can be reduced by using proper interference avoidance schemes.

In single radio access technology (single-RAT) HetCNets, interference is one of the crucial issues. In general, the interference in single-RAT HetCNets is divided into two categories, i.e., co-tier interference and cross-tier interference. Co-tier interference is caused due to overlap between

transmissions of same tier BSs to each other and their associated users. Cross-tier interference, also regarded as inter-cell interference (ICI), is defined as the overlapping of the transmissions of a BS and its associated user of one tier with the BSs and associated users of another tier [9].

CRE-based cell association expands the coverage range of sBSs and provides opportunity to a fraction of users associated with mBS, referred to as macro-cell user equipments (mUEs), to connect with the sBSs. The users associated with the sBSs after CRE employment are also referred to as range expanded users (REUs). REUs meet heavy cross-tier mBSs interference which significantly reduces performance gain. Hence, proactive interference avoidance techniques are adopted to abate such type of ICI and improve overall network performance.

Fractional frequency reuse (FFR) [10] is one of the interference mitigation techniques wherein the available spectrum is divided into multiple sub-spectra to reduce ICI and enhance coverage performance. However, this technique is spectrally inefficient due to splitting of the available spectrum. Extending the FFR technique, the authors proposed soft fractional frequency reuse (SFFR) in [11], which is spectrally more efficient than FFR. In [12], the authors proposed reverse frequency allocation (RFA) technique in which the sBSs reuse mBSs' frequency sub-bands in a multi-region environment in reverse directions.

The techniques proposed in [10]–[12] have, however, not considered load balancing [17]. Different interference avoidance strategies in conjunction with load balancing schemes have also been proposed so far in the state-of-the-art to mitigate ICI and accomplish better network performance. One of these strategies is the time domain resource partitioning [13], wherein a fraction of time slots of an mBS' frame are muted (such sub-frames are also regarded as *Almost Blank Sub-frames* (ABSs)) and are exclusively allocated to the REUs. This reduces in-band mBS interference and improves the HetCNet performance. Frequency-based resource partitioning is another strategy [14], wherein the mBS is muted on a fraction of available sub-bands, which are allocated exclusively to offloaded users. Furthermore, in [15], authors investigated SINR based analysis for resource partitioning, however, one of the key parameters, i.e., offloading, was not considered in their work. Leveraging stochastic geometry framework, Singh and Andrews [16] extended the work presented in [15], and observed the affect of joint load balancing and time-based resource partitioning on the performance metrics such as rate coverage. However, [13]–[16] considered uniform HetCNets, i.e., each tier BSs were simply uniformly distributed via homogeneous independent Poisson point processes (PPPs) in $\mathbb{R}^2$.

The homogeneous sBS distribution assumption is ill-suited in HetCNets, unless they are installed at the macro-cell edges and very large biasing is added to their transmission power. However, if the sBSs are deployed uniformly in $\mathbb{R}^2$, then it introduces the following challenges. First, sBSs closer to the mBSs result in poor offloading due to the small coverage range, (as the coverage of an sBS is a function of distance between mBS and sBS itself). Second, large biasing factor of sBS near mBS causes severe mBS interference. Third, the sBSs in less populated area result in a wastage of sBSs' resources. The analytical results of [21] and [22] depict that if sBSs are uniformly distributed then their densification does not produce any significant improvement in the coverage performance. This is due to the increased interference from more underutilized sBSs in less populated area plus interference from sBSs in adequate mBS areas where mBS provides satisfactory services to the users. Therefore, due to the above factors, uniform distribution is not a valid assumption used so far in the literature. Hence, a comprehensive non-uniform unified model is required for the evaluation of HetCNets performance with proactive load balancing and appropriate interference avoidance scheme, to obtain maximum benefits from biasing. Our work in this paper basically aims to accomplish this goal.

To reduce mBS interference for the REUs we employ the RFA technique [12] with load balancing [2], [17], while appropriately considering selective sBS deployment. In selective sBS deployment, the sBSs are deployed in the high populated area where the mBS does not provide considerable service to the users. Using such deployment along with RFA improves network performance by efficiently utilizing the small-cell resources and mitigating the cross-tier interference. In the RFA scheme, the uplink (U/L) and downlink (D/L) transmission spectra are reversed between the small-cells and macro-cells in a multi-region HetCNet. To accomplish maximum performance gain we divide the overall HetCNet region $\mathcal{S}$ into two disjoint sub-regions namely *cell-center* region, $\mathcal{S}^{(c)}$, and *cell-edge* region, $\mathcal{S}^{(o)}$. $\mathcal{S}^{(c)}$ is defined as the region around an mBS, where its coverage is acceptable; while $\mathcal{S}^{(o)}$ is defined as the region where the mBS coverage is considerably poor. Hence, to obtain maximum benefits via selective sBS deployment, we mute sBSs inside $\mathcal{S}^{(c)}$ due to the following two reasons. First, the mBS provides acceptable coverage to the users in $\mathcal{S}^{(c)}$. Second, poor offloading of users is avoided from mBS to sBSs in $\mathcal{S}^{(c)}$ due to sBSs' small coverage range. The coverage and rate performances can be further improved by keeping the average density of sBSs constant (before and after sBS muting), by deploying the same number of sBSs in $\mathcal{S}^{(o)}$ as muted in $\mathcal{S}^{(c)}$.

Based on the above discussions, our aim is to show the joint effect of RFA scheme along with load balancing on downlink SINR analysis and its derived performance metrics, such as coverage and rate, with and without considering selective sBS deployment.

A. APPROACH AND CONTRIBUTIONS

In this paper, we probabilistically analyze the coverage probability (equivalently, complementary cumulative distribution function (CCDF) of SINR threshold) and rate coverage (also regarded as CCDF of rate threshold) for a two-tier HetCNet. Fortunately, stochastic geometry [19], [20] is one of the

best analytical tools which is used comprehensively to characterize the HetCNets. The locations of both tier BSs are distributed via two independent poison point processes (PPPs). The BSs locations deployed via homogeneous PPP [21], [22], [28], provide results as accurate as the conventional hexagonal grid models [23]. Besides, stochastic geometry framework captures the randomness of the sBSs and provides analytical tractability of the performance metrics. Hence, we use stochastic geometry for the analysis of our proposed model.

The main contributions of this work are listed as follows:

1) A two-tier HetCNet with RFA employment, while taking two operating scenarios, i.e., without and with selective sBS deployments, is taken into account. In the non-selective sBS deployment scenario, sBSs are uniformly distributed via PPP and are active all the time. In the selective sBS deployment scenario, sBSs are active in the region where mBS coverage is considerably poor. In our proposed model, the sBSs are muted in $\mathcal{S}^{(c)}$ where mBS provides acceptable coverage to the users.
2) We analyze the coverage and rate performance of the proposed scenarios to observe the effect of coverage range of $\mathcal{S}^{(c)}$, user density, sBS density, and diverse bias configurations on these performance metrics.
3) Our results demonstrate that selective sBSs along with RFA employment outperform rate and coverage performances of other methods such as uniform sBS deployment along with RFA employment and the conventional CRE-only system [17] without RFA employment.
4) We also observe that retaining the average sBS density of the HetCNets (before and after muting sBSs in $\mathcal{S}^{(c)}$) further improves the performance gain of the HetCNet due to the fact that the distance between CEUs and sBSs are further reduced via sBS densification in $\mathcal{S}^{(o)}$. This encourages more CEUs to offload from mBSs to sBSs.

We hasten to add that Haenggi [29] considered deployment of sBSs at the edges of a macro-cell, while in contrast, our proposed model is based on the selective sBS deployment, in which we can select a specific area in the macro-cell besides the edges and mute the sBSs there, keeping in view the system constraints. We also discuss the CRE-based cell association along with RFA employment in a multi-region environment, while considering both uniform and selective sBS deployment.

The rest of the paper is organized as follows. Network model followed by SINR analysis, user association and load characterization are presented in Section II. Sections III and IV provide the performance analysis for the coverage probability and user rate, respectively. Numerical results are presented in Section V. Section VI concludes the paper.

II. SYSTEM MODEL

A. NETWORK MODEL AND REVERSE FREQUENCY ALLOCATION SCHEME

In the considered two-tier HetCNet, consisting of a macro-tier and a small-tier, each tier BSs' locations are randomly distributed via independent homogeneous PPPs ψ_κ, with spatial densities ξ_κ, $\forall\kappa \in \{m, s\}$ where m and s denote mBSs and sBSs, respectively. Users are also deployed through independent homogeneous PPP ψ_{u} with spatial density ξ_{u}. Transmit power of each element such as κBS and users are denoted as $\mathtt{P}_t^\kappa$ and $\mathtt{P}_t^{\mathrm{u}}$, respectively. The analysis is performed for a typical mobile user (TMU) located at origin i.e., $O = (0, 0)$, which simplifies the analysis through Slvinyak's theorem[1] [19]. We assume Rayleigh channel fading with unitary mean, i.e., $h_y = h_x \sim \exp(1)$ for both the desired and interferer channels, where y and x denote the arbitrary locations of desired and interferer links, respectively. The received powers by a TMU from a κBS in D/L and by a κBS from TMU in U/L are denoted by $\mathtt{P}^\kappa_{r,\mathrm{D/L}} = \mathtt{P}^\kappa_t \|y_\kappa\|^{-\alpha_\kappa}$ and $\mathtt{P}^\kappa_{r,\mathrm{U/L}} = \mathtt{P}^u_t \|y_\kappa\|^{-\alpha_\kappa}$, respectively. Here, $\|y_\kappa\|$ is the minimum distance between the κBS and TMU. α_κ represents the path loss exponent. The notations used in this paper are summarized in Table 1.

Using frequency division duplex (FDD) technology, transmissions in D/L and U/L directions are performed in two isolated sub-carriers. Hence, in co-channel deployed HetCNets, D/L and U/L transmissions from one tier overlap with the transmissions of the other tier resulting in heavy ICI. Using appropriate interference management schemes preserve HetCNet from such ICI. Henceforth, in our proposed model, along with flexible cell association, we use RFA as interference avoidance approach [24].

Spectrum distribution along RFA employment for the considered HetCNet is depicted in Fig. 1a. The total available band B is divided into two sub-bands, i.e., B_1 and B_2, s.t. $\mathrm{B} = \bigcup_{j=1,2} \mathrm{B}_j$, where B_1 and B_2 refer to the sub-bands allocated to the macro-cell in $\mathcal{S}^{(c)}$ and $\mathcal{S}^{(o)}$, respectively. However, each sub-band i.e., B_1 and B_2, is further divided into U/L and D/L sub-carriers, where $\mathrm{B}_1 = \mathrm{B}_{1,\mathrm{U/L}} + \mathrm{B}_{1,\mathrm{D/L}}$ and $\mathrm{B}_2 = \mathrm{B}_{2,\mathrm{U/L}} + \mathrm{B}_{2,\mathrm{D/L}}$, in $\mathcal{S}^{(c)}$ and $\mathcal{S}^{(o)}$ respectively. The macro-cell sub-bands in B_1 and B_2 are reused as the small-cell sub-bands in reverse direction as B'_1 and B'_2, respectively. Whereas, the U/L and D/L sub-carriers of the sBS in $\mathcal{S}^{(c)}$ and $\mathcal{S}^{(o)}$ are denoted as $\mathrm{B}'_2 = \mathrm{B}'_{2,u} + \mathrm{B}'_{2,\mathrm{D/L}}$ and $\mathrm{B}'_1 = \mathrm{B}'_{1,\mathrm{U/L}} + \mathrm{B}'_{1,\mathrm{D/L}}$, respectively. The mBS sub-carries in U/L and D/L directions in $\mathcal{S}^{(c)}$ are reused in reverse mode, i.e., D/L and U/L directions, by the sBS in $\mathcal{S}^{(o)}$.

The layout of the considered HetCNet with spectrum allocation, as implied in Fig. 1a, is shown in Fig. 1b. The coverages of $\mathcal{S}^{(c)}$ and $\mathcal{S}^{(o)}$ are $0 \le r \le r_1$ and $r_1 \le r \le r_2$, respectively. Using this layout, besides cross-tier interference mitigation, the spectrum based interference management also

[1] Slvinyak's theorem states that the statistics of a PPP remains unchanged if the analysis is performed on the origin.

TABLE 1. Notation summary.

Parameter	Description
ψ_m,ψ_s	PPPs of the mBSs and sBSs, respectively
ψ_u	PPP of the user locations
σ^2	Noise power at the receiver
$\gamma(.)$	SINR
$\mathrm{P}_t^m, \mathrm{P}_t^s, \mathrm{P}_t^u$	Transmit power of the serving mBS, sBSs, and users, respectively
ξ_m, ξ_s, ξ_u	Spatial densities of mBSs, sBSs, and users, respectively
$\mathrm{P}^m_{r,\mathrm{D/L}}, \mathrm{P}^s_{r,\mathrm{D/L}}$	D/L received power at user from the serving mBS and sBS, respectively
$\mathrm{P}^m_{r,\mathrm{U/L}}, \mathrm{P}^s_{r,\mathrm{U/L}}$	U/L received power from user at the serving mBS and sBS, respectively
α_m, α_s	Path loss exponents of mBSs and sBSs, respectively, where $\alpha > 2$
ζ_m , ζ_s	SINR threshold of mBSs and sBSs, respectively
$\mathcal{S}^{(c)}$, $\mathcal{S}^{(o)}$	*cell-centre* and *cell-edge* regions, respectively
Y_m,Y_s	Statistical distances from the serving mBS and serving sBSs to the TMU, respectively
W_m,W_s	Association biases of mBSs and sBSs, respectively
$h(.)$	Fading variable of the desired signal and interferers channels
$\mathrm{P}^{\mathcal{S}^{(c)}}_{\mathrm{cov},\kappa}$, $\mathrm{P}'^{\mathcal{S}^{(c)}}_{\mathrm{cov},\kappa}$	Coverage probability of a *cell-centre* TMU associated with κBS with and without selective sBS deployment, respectively
$\mathrm{P}^{\mathcal{S}^{(o)}}_{\mathrm{cov},\kappa}$, $\mathrm{P}'^{\mathcal{S}^{(o)}}_{\mathrm{cov},\kappa}$	Coverage probability of a *cell-edge* TMU associated with κBS with and without selective sBS deployment, respectively
$\mathrm{R}^{\mathcal{S}^{(c)}}_{\mathrm{rate},\kappa}$, $\mathrm{R}'^{\mathcal{S}^{(c)}}_{\mathrm{rate},\kappa}$	Rate coverage of a *cell-centre* TMU associated with κBS with and without selective sBS deployment, respectively
$\mathrm{R}^{\mathcal{S}^{(o)}}_{\mathrm{rate},\kappa}$, $\mathrm{R}'^{\mathcal{S}^{(o)}}_{\mathrm{rate},\kappa}$	Rate coverage of a *cell-edge* TMU associated with κBS with and without selective sBS deployment, respectively

improves the network spectral efficiency since it offers the same mBS spectrum to the sBS in reverse mode.

B. INTERFERENCES DISTRIBUTION IN $\mathcal{S}^{(c)}$ AND $\mathcal{S}^{(o)}$ WITHOUT AND WITH SELECTIVE sBS DEPLOYMENT

After employment of RFA scheme, interference experienced by a TMU without and with selective sBS deployment in $\mathcal{S}^{(c)}$ and $\mathcal{S}^{(o)}$ are summarized in Tables 2 and 3, respectively.

1) INTERFERENCE DISTRIBUTION WITHOUT SELECTIVE sBS DEPLOYMENT

- When a *cell-centre*-TMU, i.e., TMU $\in \mathcal{S}^{(c)}$, is associated with κBS, it experiences interference from the κBS located in $\mathcal{S}^{(c)}$ (except from the serving BS) in D/L direction and from the users associated with ωBS (i.e., ωUEs) located in $\mathcal{S}^{(o)}$ in U/L direction, s.t. $\kappa \in \{m, s\}$, $\omega \in \{m, s\}$ and $\kappa \neq \omega$.
- When κBS associated *cell-edge*-TMU, i.e., TMU $\in \mathcal{S}^{(o)}$, receives interference from the κBS located in $\mathcal{S}^{(o)}$ in D/L and from ωUEs located in $\mathcal{S}^{(c)}$ in U/L direction.

After muting sBSs in $\mathcal{S}^{(c)}$, i.e., selective sBS deployment, we assume that the users in $\mathcal{S}^{(c)}$ are served by mBSs only, however, both the mBSs and sBSs provide service to the users in $\mathcal{S}^{(o)}$.

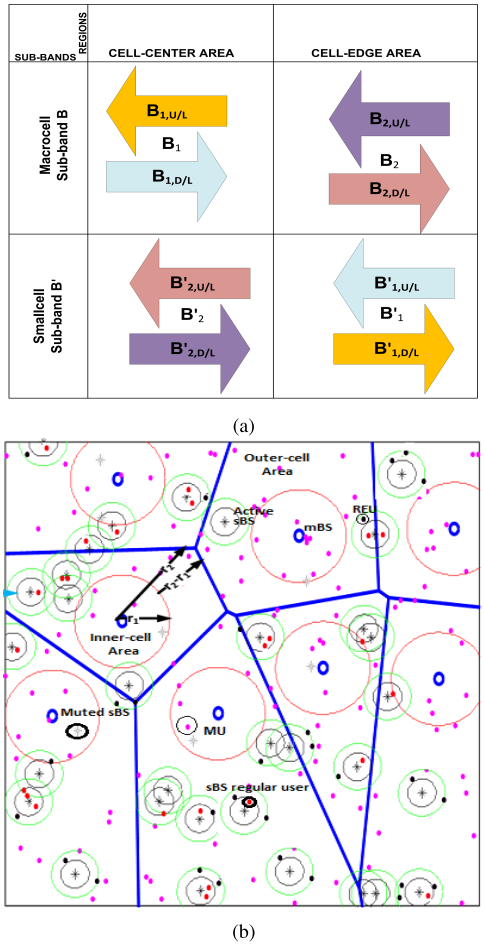

FIGURE 1. Nework Model: (1a) Spectrum distribution in RFA scheme; (1b) Network layout: $\xi_s = 5\xi_m$ and $\xi_u = 20\xi_m$.

2) INTERFERENCE DISTRIBUTION WITH SELECTIVE sBS DEPLOYMENT

- If a TMU in $\mathcal{S}^{(o)}$ is associated with mBS, it receives D/L interference from all mBSs (except serving mBS) in $\mathcal{S}^{(o)}$, however, there will be no U/L interference from sUEs in $\mathcal{S}^{(c)}$ since there is no active sBS in $\mathcal{S}^{(c)}$. As a result, selective sBS deployment further reduces interference experienced at TMU, as indicated in Table. 3.

C. SIGNAL-TO-INTERFERENCE-PLUS-NOISE RATIO ANALYSIS

1) SIGNAL-TO-INTERFERENCE-PLUS-NOISE RATIO ANALYSIS WITHOUT SELECTIVE sBS DEPLOYMENT

When TMU $\in \mathcal{S}^{(j)}$ $\forall j \in \{c, o\}$, is associated with κBS, the D/L SINR is modeled as

$$\mathrm{SINR}^{\mathcal{S}^{(j)}}_{\kappa,\mathrm{D/L}} \equiv \gamma^{\mathcal{S}^{(j)}}_{\kappa,\mathrm{D/L}} = \frac{\mathrm{P}^{\kappa}_t \mathrm{W}_\kappa h^{\mathcal{S}^{(j)}}_{y_\kappa} \|y_\kappa\|^{-\alpha_\kappa}}{\sigma^2 + \mathrm{V}^{\mathcal{S}^{(j)}}_{tot,\mathrm{D/L}}}. \quad (1)$$

Here W_κ and $h^{\mathcal{S}^{(j)}}_{y_\kappa}$ denote the biasing factor of the κBS associated user and desired channel gain in $\mathcal{S}^{(j)}$, respectively. σ^2 represents noise power received at TMU. $\mathrm{V}^{\mathcal{S}^{(j)}}_{tot,\mathrm{D/L}}$ denotes the aggregate interference received from the κBS in $\mathcal{S}^{(j)}$

TABLE 2. Interference distribution with RFA and without selective sBS deployment.

Scenario	TMU allocation	Serving BS	Interference	
			U/L	D/L
I	$\mathcal{S}^{(c)}$	mBS	sUE in $\mathcal{S}^{(o)}$	mBSs in $\mathcal{S}^{(c)}$
		sBS	mUE in $\mathcal{S}^{(o)}$	sBSs in $\mathcal{S}^{(c)}$
II	$\mathcal{S}^{(o)}$	mBS	sUEs in $\mathcal{S}^{(c)}$	mBSs in $\mathcal{S}^{(o)}$
		sBS	mUE in $\mathcal{S}^{(c)}$	sBSs in $\mathcal{S}^{(o)}$

TABLE 3. Interference distribution with RFA along with selective sBS deployment.

Scenario	TMU allocation	Serving BS	Interference	
			U/L	D/L
I	$\mathcal{S}^{(c)}$	mBS	sUE in $\mathcal{S}^{(o)}$	mBSs in $\mathcal{S}^{(c)}$
		Not exist	Not exist	Not exist
II	$\mathcal{S}^{(o)}$	mBS	Not exist	mBSs in $\mathcal{S}^{(o)}$
		sBS	mUE in $\mathcal{S}^{(c)}$	sBSs in $\mathcal{S}^{(o)}$

in D/L transmission $\mathrm{V}_{\kappa,\mathrm{D/L}}^{\mathcal{S}^{(j)}}$ and from ωUEs in $\mathcal{S}^{(i)}$ in U/L direction $\mathrm{V}_{\omega,\mathrm{U/L}}^{\mathcal{S}^{(i)}}$, where $\omega \in \{m, s\}$, $\kappa \in \{m, s\}$, $\omega \neq \kappa$ and $j \in \{c, o\}$, $i \in \{c, o\}$ $\forall j \neq i$. $\mathrm{V}_{tot,\mathrm{D/L}}^{\mathcal{S}^{(j)}}$ is written as

$$\mathrm{V}_{tot,\mathrm{D/L}}^{\mathcal{S}^{(j)}} = \mathrm{V}_{\kappa,\mathrm{D/L}}^{\mathcal{S}^{(j)}} + \mathrm{V}_{\omega,\mathrm{U/L}}^{\mathcal{S}^{(i)}}, \tag{2}$$

where $\mathrm{V}_{\kappa,\mathrm{D/L}}^{\mathcal{S}^{(j)}}$ is represented as

$$\mathrm{V}_{\kappa,\mathrm{D/L}}^{\mathcal{S}^{(j)}} = \sum_{x_l \in \psi_\kappa^{\mathcal{S}^{(j)}} \setminus y_\kappa} \mathrm{W}_\kappa \mathrm{P}_t^\kappa h_{x_l}^{\mathcal{S}^{(j)}} \|x_l\|^{-\alpha}. \tag{3}$$

Here $h_{x_l}^{\mathcal{S}^{(j)}}$ is the channel gain of κBS in $\mathcal{S}^{(j)}$. Similarly, $\mathrm{V}_{\omega,\mathrm{U/L}}^{\mathcal{S}^{(i)}}$ is denoted as

$$\mathrm{V}_{\omega,\mathrm{U/L}}^{\mathcal{S}^{(i)}} = \sum_{y_n \in \psi_\omega^{\mathcal{S}^{(i)}}} \mathrm{P}_t^u h_{y_n}^{\mathcal{S}^{(i)}} \|y_n\|^{-\alpha}, \tag{4}$$

where $h_{y_n}^{\mathcal{S}^{(i)}}$ is the channel gain of ωBS in $\mathcal{S}^{(i)}$.

Substituting (4) and (3) into (2), and then substituting the result along with value of $\mathrm{P}_{r,\mathrm{D/L}}^\kappa$ into (1) we obtain simplified form of (1).

2) SIGNAL-TO-INTERFERENCE-PLUS-NOISE RATIO ANALYSIS WITH SELECTIVE sBS DEPLOYMENT

When the TMU $\in \mathcal{S}^{(c)}$ is associated with κBS, the D/L SINR is modeled as

$$\mathrm{SINR}_{\kappa,\mathrm{D/L}}^{'\mathcal{S}^{(c)}} \equiv \gamma_{\kappa,\mathrm{D/L}}^{'\mathcal{S}^{(c)}} = \frac{\mathrm{P}_t^\kappa h_{y_\kappa}^{\mathcal{S}^{(c)}} \|y_\kappa\|^{-\alpha_\kappa}}{\sigma^2 + \mathrm{V}_{tot,\mathrm{D/L}}^{'\mathcal{S}^{(c)}}}, \tag{5}$$

where $\mathrm{V}_{tot,\mathrm{D/L}}^{'\mathcal{S}^{(c)}}$ denotes the aggregate interference received from the κBS in $\mathcal{S}^{(c)}$ in D/L transmission and from ωUEs in $\mathcal{S}^{(o)}$ in U/L direction, where $\omega \in \{m, s\}$, $\kappa \in \{m\}$, $\omega \neq \kappa$. $\mathrm{V}_{tot,\mathrm{D/L}}^{'\mathcal{S}^{(c)}}$ is written as

$$\mathrm{V}_{tot,\mathrm{D/L}}^{'\mathcal{S}^{(c)}} = \mathrm{V}_{\kappa,\mathrm{D/L}}^{'\mathcal{S}^{(c)}} + \mathrm{V}_{\omega,\mathrm{U/L}}^{'\mathcal{S}^{(o)}}, \tag{6}$$

where $\mathrm{V}_{\kappa,\mathrm{D/L}}^{'\mathcal{S}^{(c)}}$ is the D/L interference received at TMU from κBS in $\mathcal{S}^{(c)}$ (except from the serving BS). It is represented as

$$\mathrm{V}_{\kappa,\mathrm{D/L}}^{'\mathcal{S}^{(c)}} = \sum_{x_l \in \psi_\kappa^{\mathcal{S}^{(c)}} \setminus y_\kappa} \mathrm{W}_\kappa \mathrm{P}_t^m h_{x_l}^{\mathcal{S}^{(c)}} \|x_l\|^{-\alpha_\kappa}. \tag{7}$$

Similarly, $\mathrm{V}_{\omega,\mathrm{U/L}}^{'\mathcal{S}^{(o)}}$ is the total interference received at TMU in U/L direction from ωUEs located in $\mathcal{S}^{(o)}$ and can be written as

$$\mathrm{V}_{\omega,,\mathrm{U/L}}^{'\mathcal{S}^{(o)}} = \sum_{y_n \in \psi_\omega^{\mathcal{S}^{(o)}}} \mathrm{P}_t^u h_{y_n}^{\mathcal{S}^{(o)}} \|y_n\|^{-\alpha_\omega}. \tag{8}$$

Substituting (8) and (7) into (6), we get

$$\mathrm{V}_{tot,\mathrm{D/L}}^{'\mathcal{S}^{(c)}} = \sum_{x_l \in \psi_\kappa^{\mathcal{R}^{(c)}} \setminus y_\kappa} \mathrm{W}_\kappa \mathrm{P}_t^m h_{x_l}^{\mathcal{S}^{(c)}} \|x_l\|^{-\alpha} + \sum_{y_n \in \psi_\omega^{\mathcal{S}^{(o)}}} \mathrm{P}_t^u h_{y_n}^{\mathcal{S}^{(o)}} \|y_n\|^{-\alpha}, \tag{9}$$

where $\omega \in \{m, s\}$, $\kappa \in \{m\}$, $\omega \neq \kappa$. For $\kappa \in \{s\}$, since the sBSs exist only in $\mathcal{S}^{(o)}$ so $\gamma_{\kappa,\mathrm{D/L}}^{'\mathcal{S}^{(c)}} = 0$. However, for $\kappa \in \{m\}$ $\forall \kappa \neq \omega$, substituting values of $\mathrm{P}_{r,\mathrm{D/L}}^\kappa$ and (9) into (5), gives simplified form of (5).

Similarly, when TMU $\in \mathcal{S}^{(o)}$ is associated with κBS, the D/L SINR is modeled as

$$\mathrm{SINR}_{\kappa,\mathrm{D/L}}^{'\mathcal{S}^{(o)}} \equiv \gamma_{\kappa,\mathrm{D/L}}^{'\mathcal{S}^{(o)}} = \frac{\mathrm{P}_t^\kappa \mathrm{W}_\kappa h_{y_\kappa}^{\mathcal{S}^{(o)}} \|y_\kappa\|^{-\alpha_\kappa}}{\sigma^2 + \mathrm{V}_{tot,\mathrm{DL}}^{'\mathcal{S}^{(o)}}}, \tag{10}$$

where $\mathrm{W}_\kappa = 0$ for all outer-cell mBS and sBS associated regular users. However, $\mathrm{W}_\kappa > 0$ for REUs and $\mathrm{V}_{tot,\mathrm{DL}}^{\mathcal{S}^{(o)}}$ is the aggregate D/L interference received at TMU $\mathcal{S}^{(o)}$ from κBS and from ωUEs located in $\mathcal{S}^{(c)}$ in U/L direction, where $\kappa \in \{m, s\}$, $\omega \in \{m\}$, $\omega \neq \kappa$. $\mathrm{V}_{tot,\mathrm{D/L}}^{'\mathcal{S}^{(o)}}$ is now written as

$$\mathrm{V}_{tot,\mathrm{D/L}}^{'\mathcal{S}^{(o)}} = \mathrm{V}_{\kappa,\mathrm{D/L}}^{''\mathcal{S}^{(o)}} + \mathrm{V}_{\omega,\mathrm{U/L}}^{''\mathcal{S}^{(c)}}. \tag{11}$$

Here, $\mathrm{V}_{\kappa,\mathrm{D/L}}^{''\mathcal{S}^{(o)}}$ is the total D/L interference received at TMU located in $\mathcal{S}^{(o)}$ from κBS and is written as

$$\mathrm{V}_{\kappa,\mathrm{D/L}}^{''\mathcal{S}^{(o)}} = \sum_{x_l \in \psi_\kappa^{\mathcal{S}^{(o)}} \setminus y_\kappa} \mathrm{W}_\kappa \mathrm{P}_t^\kappa h_{x_l}^{\mathcal{S}^{(o)}} \|x_l\|^{-\alpha_\aleph}, \tag{12}$$

and $\mathrm{V}_{\omega,\mathrm{U/L}}^{''\mathcal{S}^{(c)}}$ is the total U/L interference received at TMU located in $\mathcal{S}^{(c)}$ from ωUEs which is given as

$$\mathrm{V}_{\omega,\mathrm{U/L}}^{''\mathcal{S}^{(c)}} = \sum_{y_n \in \psi_\omega^{\mathcal{S}^{(c)}}} \mathrm{P}_t^u h_{y_n}^{\mathcal{S}^{(c)}} \|y_n\|^{-\alpha}. \tag{13}$$

Substituting (12) and (13) into (11), we get

$$\mathrm{V}'^{\mathcal{S}^{(o)}}_{tot,\mathrm{D/L}} = \sum_{x_l \in \psi_\kappa^{\mathcal{S}^{(o)}} \setminus y_\kappa} \mathrm{W}_\kappa \mathtt{P}_t^\kappa h_{x_l}^{\mathcal{S}^{(o)}} \|x_l\|^{-\alpha} + \sum_{y_n \in \psi_\omega^{\mathcal{S}^{(c)}}} \mathtt{P}_t^u h_{y_n}^{\mathcal{S}^{(c)}} \|y_n\|^{-\alpha}. \quad (14)$$

For $\kappa \in \{s\}$ in $\mathcal{S}^{(o)}$, by substituting value of $\mathtt{P}^\kappa_{r,\mathrm{D/L}}$ and (14) into (10), we obtain $\gamma'^{\mathcal{S}^{(o)}}_{\kappa,\mathrm{D/L}}$. However, for $\kappa \in \{m\}$ in $\mathcal{S}^{(o)}$, $\sum_{y_n \in \psi_\omega^{\mathcal{S}^{(c)}}} \mathtt{P}_t^u h_{y_n}^{\mathcal{S}^{(c)}} \|y_n\|^{-\alpha} = 0$ in (14), because sBSs are muted in $\mathcal{S}^{(c)}$. Hence, (14) reduces to

$$\mathrm{V}'^{\mathcal{S}^{(o)}}_{tot,\mathrm{D/L}} = \textstyle\sum_{x_l \in \psi_\kappa^{\mathcal{S}^{(o)}} \setminus y_\kappa} \mathrm{W}_\kappa \mathtt{P}_t^\kappa h_{x_l}^{\mathcal{S}^{(o)}} \|x_l\|^{-\alpha}. \quad (15)$$

By substituting value of $\mathtt{P}^\kappa_{r,\mathrm{D/L}}$ and (15) into (10) can further simplify (10).

D. USER-BS ASSOCIATION

User-BS connectivity is based on maximum biased received power wherein the serving BS offers the maximum biased received power [14], [16], [21]. A TMU is associated with mBS if $\mathtt{P}_t^m \|y_m\|^{-\alpha_m} > \mathrm{W}_s \mathtt{P}_t^s \|y_s\|^{-\alpha_s}$, where $\{\mathtt{P}_t^m, \mathtt{P}_t^s\}$ and $\{\alpha_m, \alpha_s\}$ are the mBS and sBS transmit powers and path loss exponents, respectively. $\{\|y_m\|, \|y_s\|\}$ is the set of distances between the serving mBS or sBS and TMU, respectively. W_s is the sBS biasing factor. However, TMU otherwise associates with a sBS if it is closer to the sBS. TMU associates as an regular user or REU with sBS via unbiased cell association or biased cell association scheme, respectively, depending on the closeness to the sBS. For an unbiased sBS-TMU association, $\mathtt{P}_t^s \|y_s\|^{-\alpha_s} > \mathtt{P}_t^m \|y_m\|^{-\alpha_m}$, however, when TMU is registered as an expanded sBS user then $\mathrm{W}_s \mathtt{P}_t^s \|y_s\|^{-\alpha_s} > \mathtt{P}_t^m \|y_m\|^{-\alpha_m} > \mathtt{P}_t^s \|y_s\|^{-\alpha_s}$.

Following the maximum unbiased/biased user association scheme, a random user may associate with mBS, unbiased sBS, or biased sBS with certain probabilities, described as follows.

1) LET A_m, A_s, AND A_e DESCRIBE THE ASSOCIATION PROBABILITIES OF THE RANDOMLY SELECTED USER WITH mBS, UNBIASED sBS, AND BIASED sBS, RESPECTIVELY, WITHOUT SELECTIVE sBS DEPLOYMENT

Assuming identical path loss exponents i.e., $\alpha_m = \alpha_s = \alpha$, the association probability of user which is associated with mBS, regular sBS region, and expanded sBS region, i.e., A_m, A_s, and A_e, respectively, can be written as

$$A_m = \frac{\xi_m}{\sum_{j=m,s} \xi_j (\hat{\mathrm{W}}_j \hat{\mathtt{P}}_t^j)^{\frac{2}{\alpha}}}, \quad (16)$$

$$A_s = \frac{\xi_s}{\sum_{j=m,s} \xi_j (\hat{\mathtt{P}}_t^j)^{\frac{2}{\alpha}}}, \quad (17)$$

and

$$A_e = \frac{\xi_s}{\sum_{j=m,s} \xi_j (\hat{\mathrm{W}}_j \hat{\mathtt{P}}_t^j)^{\frac{2}{\alpha}}} - \frac{\xi_s}{\sum_{j=m,s} \xi_j (\hat{\mathtt{P}}_t^j)^{\frac{2}{\alpha}}}. \quad (18)$$

Here $\hat{\mathtt{P}}_t^j$ and $\hat{\mathrm{W}}_j$ are the ratio of the interfering BS to the serving BS transmit power and association biases, respectively. Using null probability property of PPP [19], the distribution of the statistical distances from the serving κBS i.e., $\mathrm{Y}_\kappa \ \forall \ \kappa \in \{m, s\}$, to the TMU in $\mathbb{R}^2$ is given as $f_{\mathrm{Y}_\kappa}(y_\kappa) = 2\pi\xi_\kappa y_\kappa exp(-\pi\xi_\kappa y_\kappa^2)$. Hence, (25), (17) and (18) can be obtained using unbiased mBS, unbiased sBS, and biased sBS association strategies, respectively [16].

Since users are randomly deployed via PPP ψ_u with density ξ_u, using null probability property of PPP, the probability that TMU is in $\mathcal{S}^{(o)}$ and $\mathcal{S}^{(c)}$ are $P[\mathrm{TMU} \in \mathcal{S}^{(o)}] = e^{-\xi_m \pi r_1^2}$ and $P[\mathrm{TMU} \in \mathcal{S}^{(c)}] = 1 - e^{-\xi_m \pi r_1^2}$, respectively. Conditional distributions of distances between serving κBS and TMU in $\mathcal{S}^{(c)}$ and $\mathcal{S}^{(o)}$ are $f_{Y_\kappa|\mathrm{TMU}\in\mathcal{S}^{(c)}}(y_\kappa)$ and $f_{Y_\kappa|\mathrm{TMU}\in\mathcal{S}^{(o)}}(y_\kappa)$, respectively, where $\kappa \in \{m, s\}$.

On the basis of above discussion, the conditional distance distributions of all the plausible scenarios of the proposed coverage oriented network model are described as follows.

- Distribution of distance between serving κBS, Y_κ, located at y_κ, and TMU $\in \mathcal{S}^{(c)}$ is

$$f_{Y_\kappa|\mathrm{TMU}\in\mathcal{S}^{(c)}}(y_\kappa) = \frac{f_{Y_\kappa}(y_\kappa)}{P[\mathrm{TMU} \in \mathcal{S}^{(c)}]} = \frac{2\pi\xi_\kappa y_\kappa e^{-\pi\xi_\kappa y_\kappa^2}}{1 - e^{-\xi_\kappa \pi r_1^2}}. \quad (19)$$

  Since the sBSs are inactive in $\mathcal{S}^{(c)}$, therefore, only the mBSs provide coverage to the users in $\mathcal{S}^{(c)}$, hence $\kappa \in \{m\}$. Therefore, the distance distribution of serving sBSs to the TMU $\in \mathcal{S}^{(c)}$ is 0, i.e., $f_{Y_s|\mathrm{TMU}\in\mathcal{S}^{(c)}}(y_\kappa) = 0$.
- Distance distribution between serving κBS Y_κ, located at y_κ, and TMU $\in \mathcal{S}^{(o)}$ is given as

$$f_{Y_\kappa|\mathrm{TMU}\in\mathcal{S}^{(o)}}(y_\kappa) = \frac{f_{Y_\kappa}(y_\kappa)}{P[\mathrm{TMU} \in \mathcal{S}^{(o)}]} = \frac{2\pi\xi_\kappa y_\kappa e^{-\pi\xi_\kappa y_\kappa^2}}{e^{-\xi_\kappa \pi r_1^2}}. \quad (20)$$

Here $\kappa \in \{m, s\}$ because both sBSs and mBSs are active in $\mathcal{S}^{(o)}$, and provide coverage to the users in $\mathcal{S}^{(o)}$.

The above distributions are useful in characterizing association probabilities with selective sBS deployment.

2) LET A'_m, A'_s, AND A'_e DESCRIBE THE ASSOCIATION PROBABILITIES OF THE RANDOMLY SELECTED USER WITH mBS, UNBIASED sBS, AND BIASED sBS, RESPECTIVELY, WITH SELECTIVE sBS DEPLOYMENT

Following the maximum biased association strategy, the association probabilities of the mBS and unbiased/biased sBS in selective sBS scenario with TMU are briefly elaborated below.

-Association probability, A'_m, of the TMU with mBS:

For identical path loss exponents i.e., $\alpha_m = \alpha_s = \alpha$, association probability of the TMU in $\mathbb{R}^2$ with the mBS, i.e., $A_m^{'}$, is calculated as

$$A_m^{'} = 1 - e^{-\xi_m \pi r_1^2} + \frac{\xi_m exp\left\{-\pi\left(\xi_m + \xi_s(\mathrm{W}_s \hat{\mathbb{P}}_t^s)^{\frac{2}{\alpha}}\right) r_1^2\right\}}{(\mathrm{W}_s \hat{\mathbb{P}}_t^s)^{\frac{2}{\alpha}} \xi_s + \xi_m}. \tag{21}$$

Proof: See Appendix A for proof of (21).

-Association probability, $A_s^{'}$, of TMU $\in \mathbb{R}^2$ with sBS for the same path loss exponents is given as

$$A_s^{'} = \frac{\xi_s exp\left\{-\pi\left(\xi_s + \xi_m(\hat{\mathbb{P}}_t^m)^{\frac{2}{\alpha}}\right) r_1^2\right\}}{(\hat{\mathbb{P}}_t^m)^{\frac{2}{\alpha}} \xi_m + \xi_s}. \tag{22}$$

Proof: (22) can be proved similarly as for (21). ■

-Association probability, $A_e^{'}$, of the TMU with the expanded region of sBS:

As the sBSs are active only in $\mathcal{S}^{(o)}$, for the same path loss exponents, $A_e^{'}$, can be written as (24) (given at the bottom of this page).

In the following, we characterize the load distribution of the proposed model using association probabilities derived above, which is useful in deriving the rate coverage in Section IV.

E. LOAD DISTRIBUTION

Only SINR does not captures the achieved rate of a randomly selected TMU. Load distribution also plays a vital role in rate analysis. The load associated with a particular tier BS is calculated as follows.

1) LOAD DISTRIBUTION WITHOUT CONSIDERING sBS DEPLOYMENT

Load distribution further depends on the association area. However, random sBS distribution and CRE-based cell association lead to an unknown and complex area distribution. However, due to stationary user-BS association scheme [27] the mean association area approximation of a BS of tier κ is $\frac{A_\kappa}{\xi_\kappa}$ [28]. For irregular and random cell shapes, there is no classical probability distribution function (PDF), therefore, PDF of a κBS associated area in a $2d$-plane is approximated [26] as

$$f_{A_\kappa}(a) = \frac{(\frac{7}{2})^{\frac{7}{2}}}{\Gamma(\frac{7}{2})} \left(\frac{\xi_\kappa}{A_\kappa} a\right)^{\frac{5}{2}} exp\left(-\frac{7}{2}\left(\frac{\xi_\kappa}{A_\kappa}\right) a\right), \tag{30}$$

where $\Gamma(x) = \int_0^\infty exp(-z) z^{x-1} dz$ describes the standard gamma function. The approximated association area and the estimated PDF are used to characterize the load across the κth-tier serving BS via the probability mass function (PMF) of the number of users N_κ as

$$P[\mathrm{N}_\kappa = n_\kappa] = \frac{3.5^{3.5}}{n_\kappa!} \frac{\Gamma(\kappa + 4.5)}{\Gamma(3.5)} \left(\frac{\xi_u A_\kappa}{\xi_\kappa}\right) \times \left(3.5 + \frac{\xi_u A_\kappa}{\xi_\kappa}\right)^{-(n_\kappa + 4.5)}, \quad \forall \kappa \in \{m, s, e\}. \tag{25}$$

Here $\Gamma(g) = \int_0^\infty e^{(-t)} t^{g-1} dt$ is the standard gamma distribution function.

Using (25) the load characterization of κBS in $\mathcal{S}^{(c)}$ and $\mathcal{S}^{(o)}$ with selective sBSs deployment can be obtained as following.

2) LOAD DISTRIBUTION WITH SELECTIVE sBS DEPLOYMENT

The load distribution of the serving κBS in $\mathcal{S}^{(c)}$ with selective sBS deployment is calculated as

$$P[\mathrm{N}_\kappa^{\mathcal{S}^{(c)}} = n_\kappa^{\mathcal{S}^{(c)}}] = \frac{3.5^{3.5}}{n_\kappa^{\mathcal{S}^{(c)}}!} \frac{\Gamma(n_\kappa^{\mathcal{S}^{(c)}} + 4.5)}{\Gamma(3.5)} \left(\frac{\xi_u A_\kappa^{'\mathcal{S}^{(c)}}}{\xi_\kappa}\right) \times \left(3.5 + \frac{\xi_u A_\kappa^{'\mathcal{S}^{(c)}}}{\xi_\kappa}\right)^{-(n_\kappa^{\mathcal{S}^{(c)}} + 4.5)}, \quad \forall \kappa \in \{m\}. \tag{26}$$

where $n_\kappa^{\mathcal{S}^{(c)}}$ denotes the load of κBS in $\mathcal{S}^{(c)}$ and $\kappa \in \{m\}$, since sBSs are considered inactive in $\mathcal{S}^{(c)}$, and mBS covers all the users inside this region.

Similarly, load distribution of the κBS in $\mathcal{S}^{(o)}$ with selective sBS deployment is calculated as

$$P[\mathrm{N}_\kappa^{\mathcal{S}^{(o)}} = n_\kappa^{\mathcal{S}^{(o)}}] = \frac{3.5^{3.5}}{n_\kappa^{\mathcal{S}^{(o)}}!} \frac{\Gamma(n_\kappa^{\mathcal{S}^{(o)}} + 4.5)}{\Gamma(3.5)} \left(\frac{\xi_u A_\kappa^{'\mathcal{S}^{(o)}}}{\xi_\kappa}\right) \times \left(3.5 + \frac{\xi_u A_\kappa^{'\mathcal{S}^{(o)}}}{\xi_\kappa}\right)^{-(n_\kappa^{\mathcal{S}^{(o)}} + 4.5)} \quad \forall \kappa \in \{m, s\}. \tag{27}$$

Here, $\kappa \in \{m, s\}$ because both sBSs and mBSs provide services in $\mathcal{S}^{(o)}$. $n_\kappa^{\mathcal{S}^{(o)}}$ implies the number of users associated with κBS in $\mathcal{S}^{(o)}$. The total number of associated κBS users across the HetCNet in $\mathbb{R}^2$ can, therefore, be obtained by summing (26) and (27).

Based on the mathematical preliminaries discussed in this section along with analytical framework of stochastic geometry, we evaluate the coverage SINR (also regarded as coverage probability) and rate coverage in Sections III and IV, respectively.

$$A_e^{'} \equiv A_e^{'\mathcal{S}^{(o)}} = \frac{\xi_s exp\left\{-\pi\left(\xi_s + \xi_m\left(\frac{\hat{\mathbb{P}}_t^m}{\mathrm{W}_s}\right)^{\frac{2}{\alpha}}\right) r_1^2\right\}}{(\frac{\hat{\mathbb{P}}_t^m}{\mathrm{W}_s})^{\frac{2}{\alpha}} \xi_m + \xi_s} - \frac{\xi_s exp\left\{-\pi\left(\xi_s + \xi_m(\hat{\mathbb{P}}_t^m)^{\frac{2}{\alpha}}\right) r_1^2\right\}}{(\hat{\mathbb{P}}_t^m)^{\frac{2}{\alpha}} \xi_m + \xi_s}. \tag{24}$$

$$\mathrm{P}_{\mathrm{cov},\kappa}^{\mathcal{S}^{(c)}}(\zeta_\kappa) = \frac{1}{\left(1 - e^{(-\xi_m \pi r_1^2)}\right)} \int_0^{r_1} exp\left(\frac{-\zeta_\kappa}{\mathrm{SNR}}\right) exp\left[-2\pi \times \left(\xi_\kappa^{\mathcal{S}^{(c)}} \mathrm{G}_\kappa^{\mathcal{S}^{(c)}} + \xi_u^{\mathcal{S}^{(o)}} \mathrm{G}_u^{\mathcal{S}^{(o)}}\right)\right] \left(2\pi \xi_\kappa y_\kappa e^{-\xi_\kappa \pi y_\kappa^2}\right) dy_\kappa. \quad (28)$$

$$\mathrm{P}_{\mathrm{cov},\kappa}^{\mathcal{S}^{(o)}}(\zeta_\kappa) = \frac{1}{\left(exp(-\xi_m \pi r_1^2)\right)} \int_{r_1}^{r_2} exp\left(\frac{-\zeta_\kappa}{\mathrm{SNR}}\right) exp\left[-2\pi \times \left(\xi_\kappa^{\mathcal{S}^{(o)}} \mathrm{G}_\kappa^{\mathcal{S}^{(o)}} + \xi_u^{\mathcal{S}^{(c)}} \mathrm{G}_u^{\mathcal{S}^{(c)}}\right)\right] \left(2\pi \xi_\kappa y_\kappa e^{-\xi_\kappa \pi y_\kappa^2}\right) dy_\kappa. \quad (29)$$

$$\mathrm{P}'^{\mathcal{S}^{(c)}}_{\mathrm{cov},m}(\zeta_m) = \frac{1}{\left(1 - e^{(-\xi_m \pi r_1^2)}\right)} \int_0^{r_1} exp\left(\frac{-\zeta_m}{\mathrm{SNR}}\right) exp\left[-2\pi \times \left(\xi_m^{\mathcal{S}^{(c)}} \mathrm{G}_m^{\mathcal{S}^{(c)}} + \xi_u^{\mathcal{S}^{(o)}} \mathrm{G}_u^{\mathcal{S}^{(o)}}\right)\right] \left(2\pi \xi_m y_m e^{-\xi_m \pi y_m^2}\right) dy_m. \quad (32)$$

III. COVERAGE PROBABILITY

The downlink coverage probability is defined below.

Definition 1 (Coverage Probability): The user is in coverage if the received SINR is greater than a pre-defined SINR threshold ζ.

The D/L coverage / SINR CCDF of a TMU associated with a κth-tier BS located at y is given by

$$\begin{aligned}\mathrm{P}_{\mathrm{cov}}(\zeta_\kappa) &\triangleq P(\mathrm{SINR}(y) > \zeta_\kappa) \\ &= \mathrm{E}[P(\mathrm{SINR}(y) > \zeta_\kappa)],\end{aligned}$$

and the total SINR coverage is given as

$$\mathrm{P}_{\mathrm{cov}}^{\mathrm{total}}(\zeta_\kappa) \triangleq \sum_{\kappa \in \{m,s,e\}} P(\mathrm{SINR}(y) > \zeta_\kappa) A_\kappa,$$

where A_κ is the association probability of the κth-tier serving BS.

Coverage Probability (equivalently CCDF of SINR threshold ζ) characterizes the association of a randomly located user to it serving BS such that the user is in coverage if the received SINR is greater than a pre-defined SINR threshold ζ. The SINR analysis significantly depends on the cross-tier interference between the sBSs and the overlaid mBS. Based on the mathematical preliminaries derived in Section II, tractable analysis of coverage performance of our proposed scheme, i.e., CRE-based cell association along with RFA employment, with and without selective sBS deployment assumption is presented in this section.

For a κBS-associated TMU in $\mathcal{S}^{(c)}$ and $\mathcal{S}^{(o)}$ with uniform sBS deployment, the coverage performances are calculated in Proposition 1 below.

A. COVERAGE PROBABILITY OF κBS WITHOUT SELECTIVE sBS DEPLOYMENT

Proposition 1: The coverage Probability of a TMU associated with κBS in $\mathcal{S}^{(c)}$ and $\mathcal{S}^{(o)}$ without selective sBS deployment, i.e., $\mathrm{P}_{cov,\kappa}^{\mathcal{S}^{(c)}}(\zeta_\kappa)$ and $\mathrm{P}_{cov,\kappa}^{\mathcal{S}^{(o)}}(\zeta_\kappa)$, can be calculated by (28) and (29) (on top of this page), respectively, $\forall \kappa \in \{m, s\}$.

Proof: See Appendix B for proof of (28).

Using similar mathematical approach (as adopted for (28) in Appendix VI) the coverage probability $\mathrm{P}_{cov,\kappa}^{\mathcal{S}^{(o)}}(\zeta_\kappa)$ of κBS-associated TMU in $\mathcal{S}^{(o)}$ is calculated, which is written as (29).

The following corollary provides the coverage probability for a randomly selected TMU.

Corollary 1: The CCDF of the coverage achieved at the TMU can be expressed as

$$\begin{aligned}&\mathrm{P}_{\mathrm{total\_cov}}^{\mathcal{S}}(\zeta_\kappa) \\ &= \mathrm{P}_{\mathrm{cov},\kappa}^{\mathcal{S}^{(c)}}(\zeta_\kappa) P[\mathrm{TMU} \in \mathcal{S}^{(c)}] + \mathrm{P}_{\mathrm{cov},\kappa}^{\mathcal{S}^{(o)}}(\zeta_\kappa) P[\mathrm{TMU} \in \mathcal{S}^{(o)}],\end{aligned} \quad (30)$$

For a κBS-associated TMU in $\mathcal{S}^{(c)}$ and $\mathcal{S}^{(o)}$, the coverage performances are calculated in Proposition 2 below.

B. COVERAGE PROBABILITY OF A κBS WITH SELECTIVE sBS DEPLOYMENT

Proposition 2: The coverage probability of a TMU associated with mBS and sBS in $\mathcal{S}^{(c)}$ with selective sBS deployment, $\mathrm{P}'^{\mathcal{S}^{(c)}}_{\mathrm{cov,m}}(\zeta_m)$ and $\mathrm{P}'^{\mathcal{S}^{(c)}}_{\mathrm{cov,s}}(\zeta_s)$, can be deduced from (28) as (31) and (32) (on top of this page), respectively; and the coverage probability of a TMU associated with mBS and sBS in $\mathcal{S}^{(o)}$, $\mathrm{P}'^{\mathcal{S}^{(o)}}_{\mathrm{cov,m}}(\zeta_m)$ and $\mathrm{P}'^{\mathcal{S}^{(o)}}_{\mathrm{cov,s}}(\zeta_s)$, can be deduced from (29) as (33) and (34) (on top of next page), respectively.

Based on the proposed selective sBS deployment in which the sBSs are muted in $\mathcal{S}^{(c)}$, the users connect only to the mBSs in $\mathcal{S}^{(c)}$. The coverage of sBS-associated TMU and mBS-associated TMU can be deduced from (28) as (31) (given below) and (32) (given on top of this page), respectively. Thus

$$\mathrm{P}'^{\mathcal{S}^{(c)}}_{\mathrm{cov},s}(\zeta_s) = 0. \quad (31)$$

After selective sBS deployment, coverage of *cell-edge* TMU with sBS and mBS can be deduced from (29) as (33) and (34), respectively.

The following corollary gives the coverage performance for a randomly selected TMU in co-channel deployed HetCNets.

Corollary 2: The CCDF of the SINR threshold ζ achieved at the TMU in a selective sBS deployed HetCNet,

$$\mathrm{P}'^{\mathcal{S}^{(o)}}_{\mathrm{cov},s}(\zeta_\kappa) = \frac{1}{\left(exp(-\xi_m\pi r_1^2)\right)} \int_{r_1}^{r_2} exp\left(\frac{-\zeta_s}{\mathrm{SNR}}\right) exp\left[-2\pi \times \left(\xi_s^{\mathcal{S}^{(o)}}\mathrm{G}_s^{\mathcal{S}^{(o)}} + \xi_u^{\mathcal{S}^{(c)}}\mathrm{G}_u^{\mathcal{S}^{(c)}}\right)\right]\left(2\pi\xi_s y_s e^{-\xi_s\pi y_s^2}\right) dy_s. \tag{33}$$

$$\mathrm{P}'^{\mathcal{S}^{(o)}}_{\mathrm{cov},m}(\zeta_\kappa) = \frac{1}{\left(exp(-\xi_m\pi r_1^2)\right)} \int_{r_1}^{r_2} exp\left(\frac{-\zeta_m}{\mathrm{SNR}}\right) e^{\left(-2\pi\xi_m^{\mathcal{S}^{(o)}}\mathrm{G}_m^{\mathcal{S}^{(o)}}\right)} \left(2\pi\xi_m y_m e^{-\xi_m\pi y_m^2}\right) dy_m. \tag{34}$$

$$\mathrm{R}^{\mathcal{S}^{(c)}}_{\mathrm{rate},\kappa} = \frac{1}{\left(1 - e^{(-\xi_m\pi r_1^2)}\right)} \sum_{n_\kappa^{\mathcal{S}^{(c)}}>0} \frac{3.5^{3.5}}{n_\kappa^{\mathcal{S}^{(c)}}!} \frac{\Gamma\left(n_\kappa^{\mathcal{S}^{(c)}} + 4.5\right)}{\Gamma(3.5)} \left(\frac{\xi_u A_\kappa^{\mathcal{S}^{(c)}}}{\xi_\kappa}\right) \left(3.5 + \frac{\xi_u A_\kappa^{\mathcal{S}^{(c)}}}{\xi_\kappa}\right)^{-\left(n_\kappa^{\mathcal{S}^{(c)}}+4.5\right)} \int_0^{r_1} exp\left(\frac{-\Theta(\hat{\Re}_\kappa \mathrm{N}_\kappa^{\mathcal{S}^{(c)}})}{\mathrm{SNR}}\right)$$
$$\times exp\left[-2\pi \times \left(\xi_\kappa^{\mathcal{S}^{(c)}}\mathrm{G}_\kappa^{\mathcal{S}^{(c)}} + \xi_u^{\mathcal{S}^{(o)}}\mathrm{G}_u^{\mathcal{S}^{(o)}}\right)\right]\left(2\pi\xi_\kappa y_\kappa e^{-\xi_\kappa\pi y_\kappa^2}\right) dy_\kappa, \qquad \forall\kappa \in \{m, s\}. \tag{36}$$

$$\mathrm{R}^{\mathcal{S}^{(o)}}_{\mathrm{rate},\kappa} = \frac{1}{\left(e^{(-\xi_m\pi r_1^2)}\right)} \sum_{n_\kappa^{\mathcal{S}^{(o)}}>0} \frac{3.5^{3.5}}{n_\kappa^{\mathcal{S}^{(o)}}!} \frac{\Gamma\left(n_\kappa^{\mathcal{S}^{(o)}} + 4.5\right)}{\Gamma(3.5)} \left(\frac{\xi_u A_\kappa^{\mathcal{S}^{(o)}}}{\xi_\kappa}\right) \left(3.5 + \frac{\xi_u A_\kappa^{\mathcal{S}^{(o)}}}{\xi_\kappa}\right)^{-\left(n_\kappa^{\mathcal{S}^{(o)}}+4.5\right)} \int_{r_1}^{r_2} exp\left(\frac{-\Theta(\hat{\Re}_\kappa \mathrm{N}_\kappa^{\mathcal{S}^{(o)}})}{\mathrm{SNR}}\right)$$
$$\times exp\left[-2\pi \times \left(\xi_\kappa^{\mathcal{S}^{(o)}}\mathrm{G}_\kappa^{\mathcal{S}^{(o)}} + \xi_u^{\mathcal{S}^{(c)}}\mathrm{G}_u^{\mathcal{S}^{(c)}}\right)\right]\left(2\pi\xi_\kappa y_\kappa e^{-\xi_\kappa\pi y_\kappa^2}\right) dy_\kappa, \quad \forall\kappa \in \{m, s\}. \tag{37}$$

$\mathrm{P}'^{\mathcal{S}}_{\mathrm{total\_cov}}$, can be written as

$$\mathrm{P}'^{\mathcal{S}}_{\mathrm{total\_cov}} = \left[\mathrm{P}'^{\mathcal{S}^{(c)}}_{\mathrm{cov},s} + \mathrm{P}'^{\mathcal{S}^{(c)}}_{\mathrm{cov},m}\right] \times P[\mathrm{TMU} \in \mathcal{S}^{(c)}] + \left[\mathrm{P}'^{\mathcal{S}^{(o)}}_{\mathrm{cov},s} + \mathrm{P}'^{\mathcal{S}^{(o)}}_{\mathrm{cov},m}\right] \times P[\mathrm{TMU} \in \mathcal{S}^{(o)}]. \tag{35}$$

IV. RATE COVERAGE

The coverage analysis performed in the above section is a function of distance between the TMU and the serving BS. In this section we characterize the rate coverage in $\mathcal{S}^{(c)}$ and $\mathcal{S}^{(o)}$ with and without considering selective sBS deployment.

The downlink rate coverage is defined below.

Definition 2 (Rate coverage): The rate coverage is the probability that the achievable data rate on downlink channel is greater than a pre-defined rate threshold $\Re$.

The D/L rate coverage of a TMU associated with a serving κBS located at y is given by

$$\mathrm{R}_{\mathrm{rate}} \equiv P(\mathbf{R} > \Re_\kappa) = \mathrm{E}\left[\frac{\mathrm{B}}{\mathrm{N}_\kappa}\log(1 + \mathrm{SINR}(y_\kappa)) > \Re_\kappa\right].$$

The average data rate of a TMU is given by

$$\overline{\mathrm{R}}_{\mathrm{rate}} \triangleq \sum_{\kappa\in\{m,s,e\}} A_\kappa P(\mathbf{R} > \Re_\kappa) = \sum_{\kappa\in\{m,s,e\}} A_\kappa \mathrm{E}\left[\frac{\mathrm{B}}{\mathrm{N}_\kappa}\log(1+\mathrm{SINR}(y_\kappa)) > \Re_\kappa\right],$$

where B denotes the available bandwidth and N represents the total number of users sharing the D/L resources. The rate coverage not only captures the location of the random user, it also captures the load across the serving BS.

Using Definition 2 we perform the proposed D/L analysis in Propositions 3 and 4 below, and evaluate the average user data rate of TMU, given that the TMU is associated with κBS without and with selective sBS deployment, respectively.

A. RATE COVERAGE WITHOUT SELECTIVE sBS DEPLOYMENT

Proposition 3: The rate coverage of a κBS-associated TMU in $\mathcal{S}^{(c)}$ and $\mathcal{S}^{(o)}$ without selective sBS deployment, i.e., $\mathrm{R}^{\mathcal{S}^{(c)}}_{\mathrm{rate},\kappa}$, $\mathrm{R}^{\mathcal{S}^{(o)}}_{\mathrm{rate},\kappa}$, are given as (36) and (37) (on the top of this page), respectively, $\forall\kappa \in \{m, s\}$.

Proof: See Appendix C for proof of (36).

Using similar mathematical approach (as adopted for (36) in Appendix VI) the rate coverage of κBS-associated TMU in $\mathcal{S}^{(o)}$, $\mathrm{R}^{\mathcal{S}^{(o)}}_{\mathrm{rate},\kappa}$, is calculated, which is written as (37).

The following corollary gives the user rate for a randomly selected TMU in the co-channel deployed HetCNet.

Corollary 3: The CCDF of the rate threshold $\Re$ achieved at the TMU in a co-channel HetCNet, $\mathrm{R}^{\mathcal{S}}_{\mathrm{total\_rate}}(\zeta_\kappa)$, can be written as

$$\mathrm{R}^{\mathcal{S}}_{\mathrm{total\_rate}}(\zeta_\kappa) = \mathrm{R}^{\mathcal{S}^{(c)}}_{\mathrm{rate},\kappa} P\left[\mathrm{TMU} \in \mathcal{S}^{(c)}\right] + \mathrm{R}^{\mathcal{S}^{(o)}}_{\mathrm{rate},\kappa} P\left[\mathrm{TMU} \in \mathcal{S}^{(o)}\right]. \tag{38}$$

B. RATE COVERAGE WITH SELECTIVE sBS DEPLOYMENT

Proposition 4: The rate coverage of a TMU associated with mBS and sBS in $\mathcal{S}^{(c)}$ with selective sBS deployment, i.e., $\mathrm{R}'^{\mathcal{S}^{(c)}}_{\mathrm{rate,m}}(\Re_m)$ and $\mathrm{R}'^{\mathcal{S}^{(c)}}_{\mathrm{rate,s}}(\Re_s)$, can be deduced from (36) as (39) and (40), respectively; and the rate coverage of a TMU associated with mBS and sBS in $\mathcal{S}^{(o)}$, i.e., $\mathrm{R}'^{\mathcal{S}^{(o)}}_{\mathrm{rate,m}}(\Re_m)$ and $\{\mathrm{R}'^{\mathcal{S}^{(o)}}_{\mathrm{rate,s}}(\Re_s), \mathrm{R}'^{\mathcal{S}^{(o)}}_{\mathrm{rate,e}}(\Re_s)\}$, can be deduced from (37) as (41), (42), and (43), as shown at the top of next page respectively.

Based on the proposed selective sBS deployment in which the sBSs are muted in $\mathcal{S}^{(c)}$, the basic notion behind the muting

$$\mathrm{R}'^{\mathcal{S}^{(c)}}_{\mathrm{rate},m} = \frac{1}{\left(1-e^{(-\xi_m\pi r_1^2)}\right)} \sum_{n_m^{\mathcal{S}^{(c)}}>0} \frac{3.5^{3.5}}{n_m^{\mathcal{S}^{(c)}}!} \frac{\Gamma\left(n_m^{\mathcal{S}^{(c)}}+4.5\right)}{\Gamma(3.5)} \left(\frac{\xi_u A'^{\mathcal{S}^{(c)}}_m}{\xi_m}\right) \left(3.5+\frac{\xi_u A'^{\mathcal{S}^{(c)}}_m}{\xi_m}\right)^{-\left(n_m^{\mathcal{S}^{(c)}}+4.5\right)} \int_0^{r_1} exp\left(\frac{-\Theta(\hat{\Re}_m \mathrm{N}_m^{\mathcal{S}^{(c)}})}{\mathrm{SNR}}\right)$$
$$\times exp\left[-2\pi \times \left(\xi_m^{\mathcal{S}^{(c)}} \mathrm{G}_m^{\mathcal{S}^{(c)}} + \xi_u^{\mathcal{S}^{(o)}} \mathrm{G}_u^{\mathcal{S}^{(o)}}\right)\right] \left(2\pi\xi_m y_\kappa e^{-\xi_m \pi y_m^2}\right) dy_m. \quad (40)$$

$$\mathrm{R}'^{\mathcal{S}^{(o)}}_{\mathrm{rate},s} = \frac{1}{\left(e^{(-\xi_m\pi r_1^2)}\right)} \sum_{n_s^{\mathcal{S}^{(o)}}>0} \frac{3.5^{3.5}}{n_s^{\mathcal{S}^{(o)}}!} \frac{\Gamma\left(n_s^{\mathcal{S}^{(o)}}+4.5\right)}{\Gamma(3.5)} \left(\frac{\xi_u A'^{\mathcal{S}^{(o)}}_s}{\xi_s}\right) \left(3.5+\frac{\xi_u A'^{\mathcal{S}^{(o)}}_s}{\xi_s}\right)^{-\left(n_s^{\mathcal{S}^{(o)}}+4.5\right)} \int_{r_1}^{r_2} exp\left(\frac{-\Theta(\hat{\Re}_s \mathrm{N}_s^{\mathcal{S}^{(o)}})}{\mathrm{SNR}}\right)$$
$$\times exp\left[-2\pi \times \left(\xi_s^{\mathcal{S}^{(o)}} \mathrm{G}_s^{\mathcal{S}^{(o)}} + \xi_u^{\mathcal{S}^{(c)}} \mathrm{G}_u^{\mathcal{S}^{(c)}}\right)\right] \left(2\pi\xi_s y_s e^{-\xi_s \pi y_s^2}\right) dy_s. \quad (41)$$

$$\mathrm{R}'^{\mathcal{S}^{(o)}}_{\mathrm{rate,e}} = \frac{1}{\left(e^{(-\xi_m\pi r_1^2)}\right)} \sum_{n_{\mathrm{e}}^{\mathcal{S}^{(o)}}>0} \frac{3.5^{3.5}}{n_{\mathrm{e}}^{\mathcal{S}^{(o)}}!} \frac{\Gamma\left(n_{\mathrm{e}}^{\mathcal{S}^{(o)}}+4.5\right)}{\Gamma(3.5)} \left(\frac{\xi_u A'^{\mathcal{S}^{(o)}}_{\mathrm{e}}}{\xi_s}\right) \left(3.5+\frac{\xi_u A'^{\mathcal{S}^{(o)}}_{\mathrm{e}}}{\xi_s}\right)^{-\left(n_{\mathrm{e}}^{\mathcal{S}^{(o)}}+4.5\right)} \int_{r_1}^{r_2} exp\left(\frac{-\Theta(\hat{\Re}_s \mathrm{N}_e^{\mathcal{S}^{(o)}})}{\mathrm{SNR}}\right)$$
$$\times exp\left[-2\pi \times \left(\xi_s^{\mathcal{S}^{(o)}} \mathrm{G}_s^{\mathcal{S}^{(o)}} + \xi_u^{\mathcal{S}^{(c)}} \mathrm{G}_u^{\mathcal{S}^{(c)}}\right)\right] \left(2\pi\xi_s y_s e^{-\xi_s \pi y_s^2}\right) dy_s. \quad (42)$$

$$\mathrm{R}'^{\mathcal{S}^{(o)}}_{\mathrm{rate},m} = \frac{1}{\left(e^{(-\xi_m\pi r_1^2)}\right)} \sum_{n_m^{\mathcal{S}^{(o)}}>0} \frac{3.5^{3.5}}{n_m^{\mathcal{S}^{(o)}}!} \frac{\Gamma\left(n_m^{\mathcal{S}^{(o)}}+4.5\right)}{\Gamma(3.5)} \left(\frac{\xi_u A'^{\mathcal{S}^{(o)}}_m}{\xi_m}\right) \left(3.5+\frac{\xi_u A'^{\mathcal{S}^{(o)}}_m}{\xi_m}\right)^{-\left(n_m^{\mathcal{S}^{(o)}}+4.5\right)} \int_{r_1}^{r_2} exp\left(\frac{-\Theta\left(\hat{\Re}_m \mathrm{N}_m^{\mathcal{S}^{(o)}}\right)}{\mathrm{SNR}}\right)$$
$$\times exp\left(-2\pi\xi_m^{\mathcal{S}^{(o)}} \mathrm{G}_m^{\mathcal{S}^{(o)}}\right) \left(2\pi\xi_\kappa y_m e^{-\xi_m \pi y_m^2}\right) dy_m. \quad (43)$$

of sBSs in pre-defined region is to efficiently utilize sBSs in the selected areas with poor mBS coverage. Hence the users connect only to the mBSs in $\mathcal{S}^{(c)}$ since there is no coverage of sBSs in $\mathcal{S}^{(c)}$. Thus, the rate of *cell-centre* TMU associated with sBS and mBS can be deduced from (36) as (39) and (40), respectively.

$$\mathrm{R}'^{\mathcal{S}^{(c)}}_{\mathrm{rate},\kappa} = 0. \quad (39)$$

Similarly, after selective sBS deployment, probability that a TMU $\in \mathcal{S}^{(o)}$ which is associated with an sBS and mBS accomplishes a rate greater than $\Re$ can be deduced from (37) as (41), (42), and (43), respectively. The following corollary gives the user rate for a randomly selected TMU in the co-channel deployed HetCNet.

Corollary 4: The CCDF of the rate threshold $\Re$ achieved at the TMU in a selective sBS deployed HetCNet, $\mathrm{R}'^{\mathcal{S}}_{\mathrm{total\_rate}}$, can be written as

$$\mathrm{R}'^{\mathcal{S}}_{\mathrm{total\_rate}} = \left[\mathrm{R}'^{\mathcal{S}^{(c)}}_{\mathrm{rate},m} + \mathrm{R}'^{\mathcal{S}^{(c)}}_{\mathrm{rate},s}\right] \times P[\mathrm{TMU} \in \mathcal{S}^{(c)}] + \left[\mathrm{R}'^{\mathcal{S}^{(o)}}_{\mathrm{rate},m} + \mathrm{R}'^{\mathcal{S}^{(o)}}_{\mathrm{rate},s} + \mathrm{R}'^{\mathcal{S}^{(o)}}_{\mathrm{rate},e}\right] \times P[\mathrm{TMU} \in \mathcal{S}^{(o)}]. \quad (44)$$

V. NUMERICAL RESULTS AND DISCUSSION

In this section, we provide numerical results and demonstrate the impact of RFA with and without selective sBS deployments on the network performance, and compare it with conventional HetCNet, i.e., without RFA employment. We validate our proposed model and evaluated analytical results through simulations using two-tier setting with parameters summarized in Table. 4.

TABLE 4. Simulation parameters.

Parameter	Configuration
mBSs and sBSs deployment	Two independent PPPs
Channel bandwidth	10 MHz
ξ_m	1mBS/km^2
ξ_s	$4-10$ sBSs/km^2
ξ_u	$15-50$ users/km^2
P_t^m	$40-45$ dBm
P_t^s	$20-22$ dBm
$\alpha_m = \alpha_s = \alpha$	$2.5 < \alpha \leq 4$
W_m,W_s	$\mathrm{W}_m = 0$ dB and $0 \leq \mathrm{W}_s \leq 10$ dB
σ^2	-174 dBm/Hz
Access strategy	Open access
Model type	Fully loaded

Fig. 2 shows per user average data rate (Corollaries 3 and 4) with the D/L rate distribution achieved from multiple simulations with different user density variations. It is evident from the plots that simulations results match the corresponding analytical results. However, the simulations plots deviate a little from the analytical results due to the approximations considered for the analytical tractability such as area approximation and Rayleigh fading assumption etc. It is observed that the average user

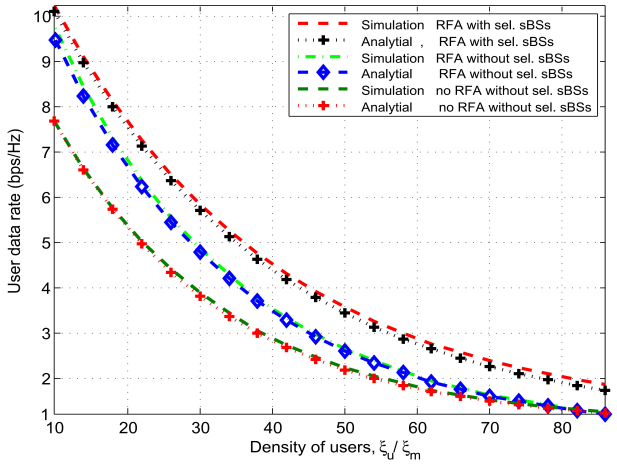

FIGURE 2. Comparison of simulation and analytical results of single user rate with user density variations: ξ_u/ξ_m, while considering effect of RFA for different schemes.

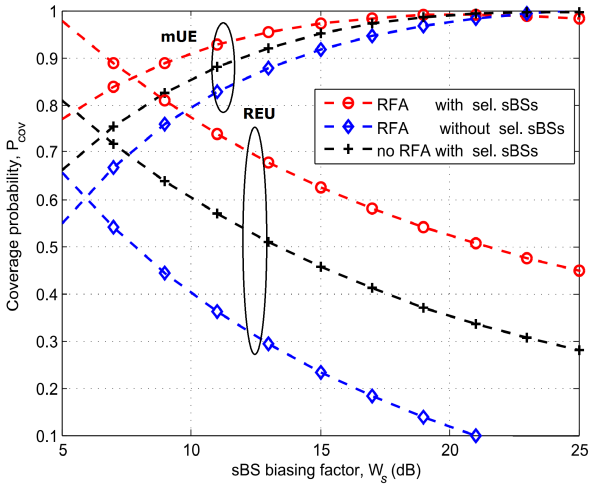

FIGURE 3. Effect of RFA with and without selective sBS deployment on coverage probability for different association bias configurations W_s.

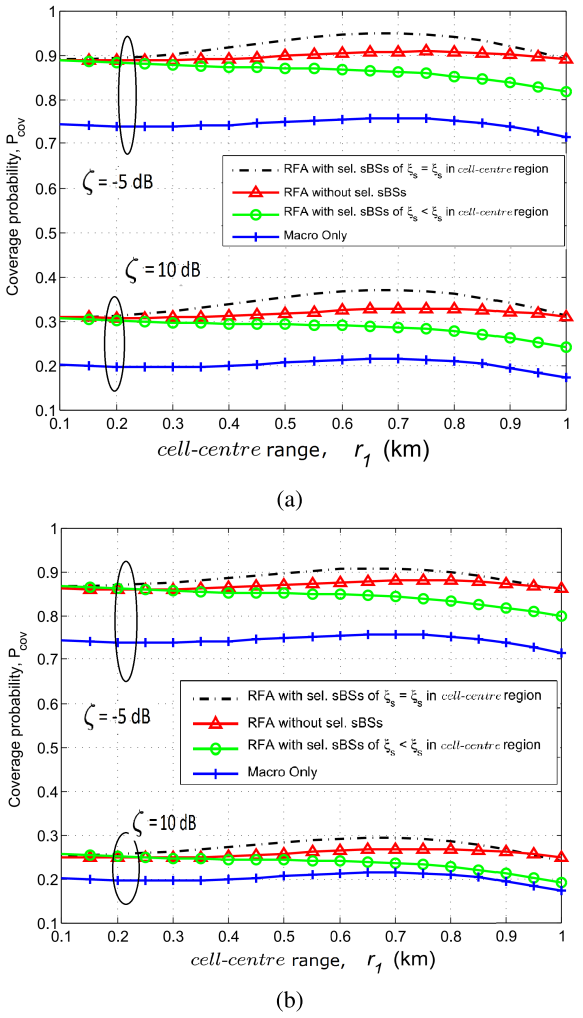

FIGURE 4. Coverage probability for different *cell − centre* ranges: (4a) impact of RFA with and without sBS deployment on coverage probability for different values of r_1, with $\zeta = -5$dB and 10dB, while $\xi_s/\xi_m = 10$; (4b) impact of RFA with and without sBS deployment on coverage probability for different values of r_1, with $\zeta = -5$dB and 10dB, while $\xi_s/\xi_m = 5$.

data rate is inversely related to user density. This is due to the fact that when user density increases, more users share the same available resources, consequently decreasing average user data rate. Hereafter, for ease of illustrations, we plot only the analytical results, however, they have also been validated by simulations.

A. COVERAGE PROBABILITY

In Figure 3, the coverage of the REU is compared against the coverage of mUE by taking into account the effect of RFA, while considering uniform and selective sBS deployment, respectively, for different bias configurations. The coverage performance of REU is inversely related to association bias, due to the fact that when biasing increases the range of sBSs increases, hence more mUEs are offloaded to sBSs. Consequently, the load of sBSs increases, hence, decrease in coverage of the REU is mainly due to the increase in its load via biasing. We can observe that the sBS deployment strategies, i.e., uniform and selective, directly impact the coverage of each user type. In the proposed model, in case of selective sBS deployment with RFA, sBSs are active in $\mathcal{S}^{(o)}$ (where the mBSs signal strength is considerably low) and most of the time available for the CEUs, hence, mBSs coverage is poor as compared to sBSs.

Fig. 4, demonstrates the coverage performance versus *cell − centre* range, i.e., r_1. From the plots we can observe the effect of $\mathcal{S}^{(c)}$ and $\mathcal{S}^{(o)}$ on coverage performance. For a suitable range of $\mathcal{S}^{(c)}$ the coverage of non-selective sBS deployed HetCNet is approximately the same as that of the selective sBSs deployed HetCNet (with muted sBSs in $\mathcal{S}^{(c)}$), even for 50% of the total number of sBSs. For example, in Fig. 4a, the coverage performance of the non selective sBSs at $r_1 = 0.5$ km, is relatively the same as for the deactivated sBSs' scenario. This means that the same coverage can be achieved

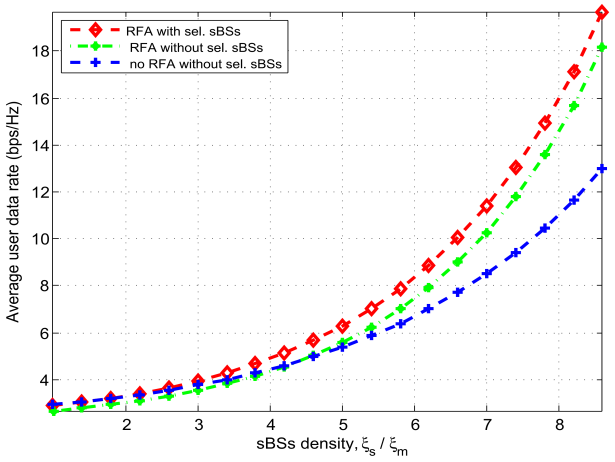

FIGURE 5. Average user data rate vs sBS density.

with a considerably lower de facto sBS density. However, deploying the same number of sBSs in $\mathcal{S}^{(o)}$ as muted in $\mathcal{S}^{(c)}$ to keep the total sBSs active in $\mathcal{S}^{(o)}$ further improves the coverage performance. For instance, taking the upper set of plots in Fig. 4a, the coverage of the selective sBS deployed HetCNet is 94.3% at $r_1 = 0.5$ km, compared with uniform sBS deployed HetCNet and macro-cellular network which are 90.4% and 75.48%, respectively. Similar improvements can be also be observed in Fig. 4b, with different ξ_s and different ζ.

B. COVERAGE RATE

In Fig. 5, we illustrate the effect of sBS density on user rate in 25-users system, i.e., $\xi_u = 25\xi_m$. It is observed that the user data rate increases as the sBS density increases. However, as the sBS density increases the number of associated users to sBSs, i.e., sUEs, decreases, since a large fraction of resources offer services to less no of sUEs. It can be observed that the user data rate achieved by the proposed model with selective sBS deployment outperforms other methods. It is also evident from the plots that for a small sBS density, i.e., $2-4$ sBSs, the user data rate of the proposed scheme without sBS deployment is better than the selective one. This is due to the fact that when the sBS density is small, load balancing is inappropriate in HetCNets and the users associate with mBS having high data rate.

Fig. 6 shows the relation between the user data rate and biasing factor, while considering small and large user densities. It is observed in Fig. 6a, that, in case of high user density, more mUEs are offloaded to sBSs, which degrades the data rate of the unbiased sBS users because sBS resources are more utilized. However, the average user data rate is improved because of improvement in the data rate of offloaded mUEs, which are mostly located at cell edge where the mBS signal power is considerably low. Furthermore, the optimal bias value decreases as the user density

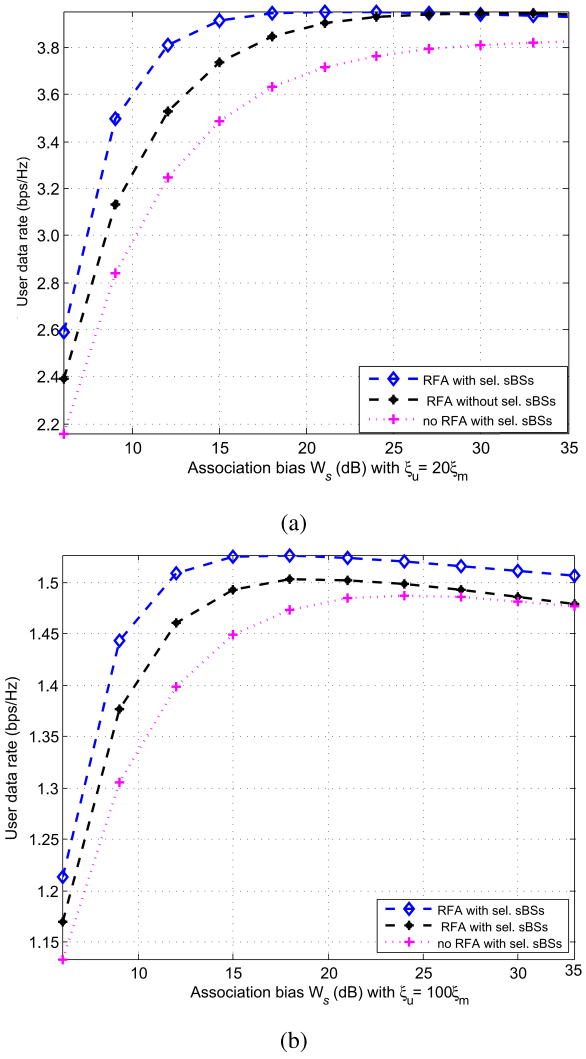

FIGURE 6. Average per user data rate for different association bias configurations: (6a) impact of RFA with and without sBS deployment on average user data rate for different values of ζ, with $\xi_u = 20\xi_m$; (6b) impact of RFA with and without sBS deployment on average user data rate for different values of ζ, with $\xi_u = 100\xi_m$.

increases due to the fact that in case of heavy load more users with lower SINR (users with lower maximum received power from the closest sBS than that of the nearest mBS) are offloaded to sBSs. For instance, the optimal value for the selective sBS deployment with RFA employment is observed in Fig. 6a (lightly loaded) and Fig. 6b (heavily loaded) to be 18 dB and 15 dB, respectively.

Fig. 7 illustrates the effect on user data rate for different association bias configurations of sBSs. The per user data rate increases as the sBS density increases due to the fact that for a constant user density, when the sBS density increases, the number of associated user to sBSs, i.e., sUEs, decreases. Thus a larger number of sBSs provide service to fewer number of sUEs. For instance, for a constant association bias, i.e., 18 dB, the data rates at $\xi_s = 3\xi_m$ and $\xi_s = 6\xi_m$ are > 2.5 bps/Hz and < 1.9 bps/Hz, respectively.

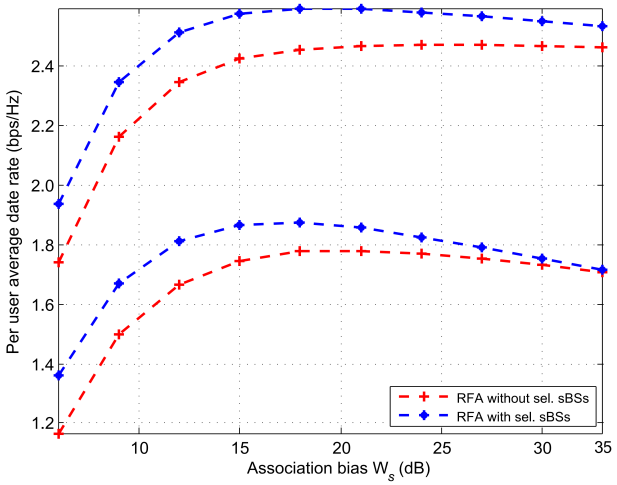

FIGURE 7. Effect of RFA, with and without selective sBS deployment, on rate for different association bias configurations W_s with $\xi_s = 3\xi_m$ (lower plots) and $\xi_s = 6\xi_m$ (upper plots).

VI. CONCLUSION

In our proposed model we probabilistically analyse the coverage probability and user rate for the joint effect of RFA employment and load balancing in a HetCNet. We observe the effect of association bias and RFA employment over the coverage and rate with and without considering selective sBS deployment. It is clear from the numerical results that the coverage and rate improve with the employment of RFA since it abates the ICI of mBS on offloaded users. It was also observed that if CRE is reinforced by RFA scheme, it can improve the rate performance efficiently. Selective sBS deployment can further improve the coverage and the rate significantly. Our results demonstrate that even by muting 50% of sBSs in a predefined region, (where the mBS power is considerably low) we can achieve nearly the same coverage as uniformly deployed sBSs. Furthermore, by properly selecting the important parameters such as *cell-center* range and biasing factor, for the selective sBS deployment, the coverage can be significantly improved at no extra cost of resources.

APPENDIX A
PROOF OF (21)

The mBSs offer service to the users located in $\mathcal{S}^{(c)}$ and $\mathcal{S}^{(o)}$, so we can write

$$A_m^{'} = A_m^{'\mathcal{S}^{(c)}} + A_m^{'\mathcal{S}^{(o)}}, \tag{45}$$

where, $A_m^{'\mathcal{S}^{(c)}}$ and $A_m^{'\mathcal{S}^{(o)}}$ are the association probabilities of mBS with TMU in $\mathcal{S}^{(c)}$ and $\mathcal{S}^{(o)}$, respectively.
Now

$$A_m^{'\mathcal{S}^{(c)}} \overset{(i)}{\equiv} P[\Phi = m,\ \text{TMU} \in S^{(c)}] = 1 - e^{-\xi_m \pi r_1^2}. \tag{46}$$

In (46), the values of Φ denote the type of BS to which the TMU associates. For the proposed network model, $\Phi = \{m\}$ and $\Phi = \{s\}$ express TMU association with mBS and sBS, respectively. Step (i) comes from the selective sBS deployment assumption where the sBSs in $\mathcal{S}^{(c)}$ are muted and the users in $\mathcal{S}^{(c)}$ are serviced only by the mBSs.

Similarly, the association probability of mBS with TMU in $\mathcal{S}^{(o)}$, i.e., $A_m^{'\mathcal{S}^{(o)}}$ is given as

$$A_m^{'\mathcal{S}^{(o)}} = \frac{\xi_m exp\left\{-\pi\left(\xi_m + \xi_s(\mathrm{W}_s\hat{\mathrm{P}}_t^s)^{\frac{1}{\alpha}}\right) r_1^2\right\}}{\xi_m + (\mathrm{W}_s\hat{\mathrm{P}}_t^s)^{\frac{2}{\alpha}}\xi_s}. \tag{47}$$

We prove (47) below. *Proof:*

$$A_m^{'\mathcal{S}^{(o)}} = P[\Phi = m, \text{TMU} \in S^{(o)}].$$

Using Bayes' theorem

$$A_m^{'\mathcal{S}^{(o)}} = P[\Phi = m|\text{TMU} \in S^{(o)}] = P[\text{TMU} \in S^{(o)}], \tag{48}$$

where

$$\begin{aligned} &P[\Phi = m|\text{TMU} \in S^{(o)}] \\ &= E_{Y_m}[P[\Phi = m|\text{TMU} \in S^{(o)}, Y_m = y]] \\ &= \int_{r_1}^{\infty} P[\Phi = m|\text{TMU} \in S^{(o)}, Y_m = y_m] \\ &\quad \times f_{Y_m|\text{TMU}\in S^{(o)}}(y_m)dy_m. \end{aligned} \tag{49}$$

Here y_m is the minimum distance between the TMU and the associated serving mBS. Under the maximum power received strategy, $\mathrm{P}^m_{r,\mathrm{D/L}} > \mathrm{P}^s_{r,\mathrm{D/L}}$. Thus

$$\begin{aligned} &P[\Phi = m|\text{TMU} \in S^{(o)}, Y_m = y_m] \\ &= P[\mathrm{P}^m_{r,\mathrm{D/L}} > \mathrm{P}^s_{r,\mathrm{D/L}}] \\ &= P\left[y_s > (\mathrm{W}_s\hat{\mathrm{P}}_t^s)^{\frac{1}{\alpha_s}} y_m^{\frac{1}{\hat{\alpha}_s}}\right], \end{aligned} \tag{50}$$

where $\hat{\alpha}_s$ and $\hat{\mathrm{P}}_t^s$ are the path loss exponent and transmit power ratios of the interfering sBS to the serving mBS, respectively, i.e., $\hat{\alpha}_s = \frac{\alpha_s}{\alpha_m}$ and $\hat{\mathrm{P}}_t^s = \frac{\mathrm{P}_t^s}{\mathrm{P}_t^m}$. $\mathrm{P}^m_{r,\mathrm{D/L}} = \mathrm{P}_t^m\|y_m\|^{-\alpha_m}$ and $\mathrm{P}^s_{r,\mathrm{D/L}} = \mathrm{W}_s\mathrm{P}_t^s\|y_s\|^{-\alpha_s}$, are the D/L received powers from mBS and sBS at TMU, respectively.

Using null probability property of PPP, (50) can be written as

$$P\left[y_s > (\mathrm{W}_s\hat{\mathrm{P}}_t^s)^{\frac{1}{\alpha_s}} y_m^{\frac{1}{\hat{\alpha}_s}}\right] = e^{\left(-\pi\xi_s\left((\mathrm{W}_s\hat{\mathrm{P}}_t^s)^{\frac{1}{\alpha_s}} y^{\frac{1}{\hat{\alpha}_s}}\right)^2\right)}. \tag{51}$$

Substituting (20) and (51) into (49) along with identical path loss exponents, i.e., $\alpha_m = \alpha_s = \alpha$, and after performing a few algebraic manipulations we obtain (47). This completes the proof of (47).

Furthermore, substituting (46) and (47) into (45), we can reach the required result (21). ■

APPENDIX B
PROOF OF PROPOSITION 1

Proof:

$$\begin{aligned} &\mathrm{P}_{\mathrm{cov},\kappa}^{\mathcal{S}^{(c)}}(\zeta_\kappa) \\ &= \mathrm{E}\left[P\left[\gamma_{\kappa,\mathrm{D/L}}^{\mathcal{S}^{(c)}}(y_\kappa) > \zeta_\kappa|\text{TMU} \in \mathcal{S}^{(c)}\right]\right] \\ &= \int_0^{r_1} P\left[\gamma_{\kappa,\mathrm{D/L}}^{\mathcal{S}^{(c)}}(y_\kappa) > \zeta_\kappa|\text{TMU} \in \mathcal{S}^{(c)}\right] \\ &\quad \times f_{Y_\kappa|\text{TMU}\in\mathcal{S}^{(c)}}(y_\kappa)dy_\kappa, \end{aligned} \tag{52}$$

where γ_κ and ζ_κ are the SINR and its threshold of the κBS respectively. $P[\gamma^{\mathcal{S}^{(c)}}_{\kappa,\mathrm{D/L}}(y_\kappa) > \zeta_\kappa|\mathrm{TMU} \in \mathcal{S}^{(c)}]$ is the success probability given that TMU $\in \mathcal{S}^{(c)}$ is associated with κBS, and can be calculated as

$$\begin{aligned} &P\left[\gamma^{\mathcal{S}^{(c)}}_{\kappa,\mathrm{D/L}}(y_\kappa) > \zeta_\kappa|\mathrm{TMU} \in \mathcal{S}^{(c)}\right] \\ &\overset{(ii)}{=} exp\left(\frac{-\zeta_\kappa}{\mathrm{SNR}}\right)\mathrm{E}_{\mathrm{V}^{\mathcal{S}^{(c)}}_{tot,\mathrm{D/L}}}\left[e^{\left(-s\mathrm{V}^{\mathcal{S}^{(c)}}_{tot,\mathrm{D/L}}\right)}\right] \\ &\overset{(iii)}{=} exp\left(\frac{-\zeta_\kappa}{\mathrm{SNR}}\right)\mathrm{M}_{\mathrm{V}^{\mathcal{S}^{(c)}}_{tot,\mathrm{D/L}}}(s), \end{aligned} \tag{53}$$

where $s = \frac{\zeta_\kappa \|y_\kappa\|^\alpha}{\mathrm{P}^\kappa_t}$. Step (ii) in (53) comes from the Rayleigh fading assumption for all the links having unitary mean value, i.e., $h^{\mathcal{S}^{(c)}}_y(.) \sim exp(1)$ and the independence assumption of interference. $\mathrm{E}_{\mathrm{V}^{\mathcal{S}^{(c)}}_{tot,\mathrm{D/L}}}$ is the expectation of the commutative interference $\mathrm{V}^{\mathcal{S}^{(c)}}_{tot,\mathrm{D/L}}(.)$. In Step (iii), $\mathrm{M}_{\mathrm{V}^{\mathcal{S}^{(c)}}_{tot,\mathrm{D/L}}}(s)$ is the Moment Generating Function (MGF) [19] of the commutative interference $\mathrm{V}^{\mathcal{S}^{(c)}}_{tot,\mathrm{D/L}}(.)$, given in (2), which can be calculated as

$$\begin{aligned} &\mathrm{M}_{\mathrm{V}^{\mathcal{S}^{(c)}}_{tot,\mathrm{D/L}}}(s) \\ &= \mathrm{E}_{\psi^{\mathcal{S}^{(o)}}_\kappa,\psi^{\mathcal{S}^{(o)}}_u,h_{x_l},h_{y_n}}\Bigg[exp\Bigg(-s\Bigg(\sum_{x_l\in\psi^{\mathcal{S}^{(c)}}_\kappa\setminus y_\kappa}\mathrm{W}_\kappa \mathrm{P}^\kappa_t h^{\mathcal{S}^{(c)}}_{x_l}\|x_l\|^{-\alpha} \\ &\qquad + \sum_{y_n\in\psi^{\mathcal{S}^{(o)}}_u}\mathrm{P}^u_t h^{\mathcal{S}^{(o)}}_{y_n}\|y_n\|^{-\alpha}\Bigg)\Bigg)\Bigg], \end{aligned} \tag{54}$$

where $\mathrm{W}_\kappa = 0,\ \forall\kappa \in \{m,s\}$, (i.e., regular users associated with mBSs and sBSs) and $\mathrm{W}_\kappa > 0,\ \forall\kappa \in \{e\}$, (i.e., REUs only.) x_l and y_n are the arbitrary locations of the κBS (other than the serving kBS) in $\mathcal{S}^{(c)}$ in D/L directions and random users locations in $\mathcal{S}^{(o)}$, respectively.

Using independence assumptions of the PPPs $\psi^{\mathcal{S}^{(c)}}_\kappa$ and $\psi^{\mathcal{S}^{(o)}}_u$, and the fading coefficients $h^{\mathcal{S}^{(c)}}_{x_l}$ and $h^{\mathcal{S}^{(o)}}_{y_n}$, (54) can be further simplified in Step (iv) below as

$$\begin{aligned} &\mathrm{M}_{\mathrm{V}^{\mathcal{S}^{(c)}}_{tot,\mathrm{D/L}}}(s) \\ &\overset{(iv)}{=} \mathrm{E}_{\psi^{\mathcal{S}^{(c)}}_\kappa}\left[\prod_{x_l\in\psi^{\mathcal{S}^{(c)}}_\kappa\setminus y_\kappa}\mathrm{M}_{h^{\mathcal{S}^{(c)}}_{x_l}}(\mathrm{W}_\kappa s\mathrm{P}^u_t\|x_l\|^{-\alpha})\right] \\ &\quad\times\mathrm{E}_{\psi^{\mathcal{S}^{(o)}}_u}\left[\prod_{y_n\in\psi^{\mathcal{S}^{(o)}}_u}\mathrm{M}_{h^{\mathcal{S}^{(o)}}_{y_n}}(s\mathrm{P}^u_t\|y_n\|^{-\alpha})\right] \\ &= exp\left(-2\pi\xi^{\mathcal{S}^{(c)}}_\kappa\int_{y'_\kappa}^{r_1}\left\{1-\mathrm{M}_{h^{\mathcal{S}^{(c)}}_{x_l}}(\mathrm{W}_\kappa s\mathrm{P}^\kappa_t\|x_l\|^{-\alpha})\right\}x_l dx_l\right) \\ &\quad\times exp\left(-2\pi\xi^{\mathcal{S}^{(o)}}_d\int_{r_1}^{r_2}\left\{1-\mathrm{M}_{h^{\mathcal{S}^{(o)}}_{y_n}}(s\mathrm{P}^u_t\|y_n\|^{-\alpha})\right\}y_n dy_n\right). \end{aligned} \tag{55}$$

Here $\mathrm{M}_{h^{\mathcal{S}^{(c)}}_{y_n}}(.)$ and $\mathrm{M}_{h^{\mathcal{S}^{(o)}}_{y_n}}(.)$ are the MGFs of the interfering fading coefficients kBS) in $\mathcal{S}^{(c)}$ in D/L directions and random users locations in $\mathcal{S}^{(o)}$, respectively. Using Rayleigh fading assumption, (55) is further simplified as

$$\begin{aligned} &\mathrm{M}_{\mathrm{V}^{\mathcal{S}^{(c)}}_{tot,\mathrm{D/L}}}(s) \\ &= exp\left(-2\pi\xi^{\mathcal{S}^{(c)}}_\kappa\int_{y'_\kappa}^{r_1}\frac{x_l}{1+(s\mathrm{W}_\kappa\mathrm{P}^\kappa_t)^{-1}x_l^\alpha}dx_l\right) \\ &\quad\times exp\left(-2\pi\xi^{\mathcal{S}^{(o)}}_d\int_{r_1}^{r_2}\frac{y_n}{1+(s\mathrm{P}^u_t)^{-1}y_n^\alpha}dy_n\right), \end{aligned} \tag{56}$$

where, y'_κ denotes the nearest κBS interferer distance and can be obtained as described below.

-If an ith-region TMU, i.e., $\{\mathrm{TMU} \in \mathcal{S}^{(i)}\}_{i=c,o}$ is associated with the κBS located at y_κ, following D/L association rules y'_κ is calculated as

$$\begin{aligned} \mathrm{P}^\kappa_{r,\mathcal{S}^{(i)}} &> \mathrm{P}^\omega_{r,\mathcal{S}^{(i)}}\ \forall\ \mathrm{W}_\kappa,\ \mathrm{W}_\omega \geq 1 \\ &\Longrightarrow \mathrm{W}_\kappa\mathrm{P}^\kappa_t y_\kappa^{-\alpha} > \mathrm{W}_\omega\mathrm{P}^\omega_t y_\kappa'^{-\alpha} \\ &\Longrightarrow y'_\kappa > \left(\frac{\mathrm{W}_\omega\mathrm{P}^\omega_t}{\mathrm{W}_\kappa\mathrm{P}^\kappa_t}\right)^{\frac{1}{\alpha}}y_\kappa, \end{aligned} \tag{57}$$

where $\kappa \in \{m,s\}$, $\omega \in \{m,s\}$ $\forall\kappa \neq \omega$. By substituting $a \equiv (s\mathrm{W}_\kappa\mathrm{P}^\kappa_t)^{\frac{2}{\alpha}}x_l^2$ and $b \equiv (s\mathrm{P}^u_t)^{\frac{2}{\alpha}}y_n^2$, (56) can be further simplified as

$$\mathrm{M}_{\mathrm{V}^{\mathcal{S}^{(c)}}_{tot,\mathrm{D/L}}}(s) = exp\left(-2\pi\left[\xi^{\mathcal{S}^{(c)}}_\kappa \mathrm{G}^{\mathcal{S}^{(c)}}_\kappa + \xi^{\mathcal{S}^{(o)}}_u \mathrm{G}^{\mathcal{S}^{(o)}}_u\right]\right), \tag{58}$$

where

$$\mathrm{G}^{\mathcal{S}^{(c)}}_\kappa = \int_{y'_\kappa}^{r_1}\frac{x_l dx_l}{1+(s\mathrm{W}_\kappa\mathrm{P}^\kappa_t)^{-1}\|x_l\|^\alpha} = y_\kappa^{\frac{2}{\alpha}}\int_{y_\kappa^{\frac{-2}{\alpha}}}^{r_1}\frac{a}{1+a^{\frac{\alpha}{2}}}da,$$

and

$$\mathrm{G}^{\mathcal{S}^{(o)}}_u = \int_{r_1}^{r_2}\frac{y_n dy_n}{1+(s\mathrm{P}^u_t)^{-1}\|y_n\|^\alpha} = y_\kappa^{\frac{2}{\alpha}}\int_{r_1}^{r_2}\frac{b}{1+b^{\frac{\alpha}{2}}}db.$$

Finally, substituting (58) into (53) success probability is obtained as

$$\begin{aligned} &P[\gamma^{\mathcal{S}^{(c)}}_{\kappa,\mathrm{D/L}}(y_\kappa) > \zeta_\kappa|\mathrm{TMU} \in \mathcal{S}^{(c)}] \\ &= exp\left(\frac{-\zeta_\kappa}{\mathrm{SNR}}\right)exp\left(-2\pi\left[\xi^{\mathcal{S}^{(c)}}_\kappa \mathrm{G}^{\mathcal{S}^{(c)}}_\kappa + \xi^{\mathcal{S}^{(o)}}_u \mathrm{G}^{\mathcal{S}^{(o)}}_u\right]\right). \end{aligned} \tag{59}$$

Substituting (19) and (59) into (52) completes the proof of (28). ■

APPENDIX C
PROOF OF PROPOSITION 3

Proof:

$$\mathrm{R}^{\mathcal{S}^{(c)}}_{\mathrm{rate},\kappa} = P(\mathbf{R}^{\mathcal{S}^{(c)}}_\kappa > \Re_\kappa|\mathrm{TMU} \in \mathcal{S}^{(c)}), \tag{60}$$

where $\mathbf{R}^{\mathcal{S}^{(c)}}_\kappa$ and $\Re_\kappa$ are the achievable rate by the TMU when it is associated with the κBS and the rate threshold of the κBS, respectively. Using the Shannon capacity theorem, $\mathbf{R}^{\mathcal{S}^{(c)}}_\kappa$ can be calculated as

$$\mathbf{R}^{\mathcal{S}^{(c)}}_\kappa = \frac{\mathrm{B}}{\mathrm{N}^{\mathcal{S}^{(c)}}_\kappa}\log\left(1+\gamma^{\mathcal{S}^{(c)}}_{\kappa,\mathrm{D/L}}\right), \tag{61}$$

where B and $\mathrm{N}_{\kappa}^{\mathcal{S}^{(c)}}$ denote the available bandwidth and the number of total associated users (TMU plus others) with the serving κBS in $\mathcal{S}^{(c)}$, respectively. Substituting (61) into (60), we get

$$\begin{aligned}
\mathrm{R}_{\mathrm{rate},\kappa}^{\mathcal{S}^{(c)}} &= P\left[\frac{\mathrm{B}}{\mathrm{N}_{\kappa}^{\mathcal{S}^{(c)}}}\log\left(1+\gamma_{\kappa,\mathrm{D/L}}^{\mathcal{S}^{(c)}}\right) > \Re_{\kappa}|\mathrm{TMU}\in\mathcal{S}^{(c)}\right] \\
&= \mathrm{E}_{\mathrm{N}_{\kappa}^{\mathcal{S}^{(c)}}}\left[\gamma_{\kappa,\mathrm{D/L}}^{\mathcal{S}^{(c)}} > e^{\frac{\Re_{\kappa}\mathrm{N}_{\kappa}^{\mathcal{S}^{(c)}}}{\mathrm{B}}-1}|\mathrm{TMU}\in\mathcal{S}^{(c)}\right] \\
&\overset{(v)}{=} \mathrm{E}_{\mathrm{N}_{\kappa}^{\mathcal{S}^{(c)}}}\left[\mathrm{P}_{\mathrm{cov},\kappa}^{\mathcal{S}^{(c)}}\left(e^{\frac{\Re_{\kappa}\mathrm{N}_{\kappa}^{\mathcal{S}^{(c)}}}{\mathrm{B}}-1}\right)\right] \\
&\overset{(vi)}{=} \mathrm{E}_{\mathrm{N}_{\kappa}^{\mathcal{S}^{(c)}}}\left[\mathrm{P}_{\mathrm{cov},\kappa}^{\mathcal{S}^{(c)}}\left(e^{\hat{\Re}_{\kappa}\mathrm{N}_{\kappa}^{\mathcal{S}^{(c)}}}-1\right)\right] \\
&\overset{(vii)}{=} \mathrm{E}_{\mathrm{N}_{\kappa}^{\mathcal{S}^{(c)}}}\left[\mathrm{P}_{\mathrm{cov},\kappa}^{\mathcal{S}^{(c)}}\left(\Theta\left(\hat{\Re}_{\kappa}\mathrm{N}_{\kappa}^{\mathcal{S}^{(c)}}\right)\right)\right], \qquad (62)
\end{aligned}$$

where Step (v) is obtained from (28), $\hat{\Re}_{\kappa} = \frac{\Re_{\kappa}}{\mathrm{B}}$ in Step (vi), and $\Theta(\hat{\Re}_{\kappa}\mathrm{N}_{\kappa}^{\mathcal{S}^{(c)}}) = e^{\hat{\Re}_{\kappa}\mathrm{N}_{\kappa}^{\mathcal{S}^{(c)}}} - 1$ in Step (vii).

We can write the right side of (62) as

$$\begin{aligned}
&\mathrm{E}_{\mathrm{N}_{\kappa}^{\mathcal{S}^{(c)}}}\left[\mathrm{P}_{\mathrm{cov},\kappa}^{\mathcal{S}^{(c)}}\left(\Theta\left(\hat{\Re}_{\kappa}\mathrm{N}_{\kappa}^{\mathcal{S}^{(c)}}\right)\right)\right] \\
&\quad= \sum_{n_{\kappa}^{\mathcal{S}^{(c)}}>0} P\left[\mathrm{N}_{\kappa}^{\mathcal{S}^{(c)}} = n_{\kappa}^{\mathcal{S}^{(c)}}\right]\mathrm{P}_{\mathrm{cov},\kappa}^{\mathcal{S}^{(c)}}\Theta\left(\hat{\Re}_{\kappa}\mathrm{N}_{\kappa}^{\mathcal{S}^{(c)}}\right). \qquad (63)
\end{aligned}$$

Now combining (46) with (28), replacing ζ_{κ} by $\Theta\left(\hat{\Re}_{\kappa}\mathrm{N}_{\kappa}^{\mathcal{S}^{(c)}}\right)$ and then substituting the result into (63), we reach (36). ■

Acknowledgment

A part of this paper has been presented in the 27th Annual IEEE International Symposium on Personal, Indoor and Mobile Radio Communications (PIMRC2016): Mobile and Wireless Networks in Valencia, Spain [1].

REFERENCES

[1] F. Muhammad, Z. H. Abbas, and L. Jiao, "Analysis of interference avoidance with load balancing in heterogeneous cellular networks," in *Proc. 27th Annu. IEEE Int. Symp. Pers., Indoor Mobile Radio Commun. (PIMRC)*, Valencia, Spain. Sep. 2016, pp. 1–6.

[2] A. Ghosh *et al.*, "Heterogeneous cellular networks: From theory to practice," *IEEE Commun. Mag.*, vol. 50, no. 6, pp. 54–64, Jun. 2012.

[3] Y. Deng, L. Wang, M. Elkashlan, M. Di Renzo, and J. Yuan, "Modeling and analysis of wireless power transfer in heterogeneous cellular networks," *IEEE Trans. Commun.*, vol. 64, no. 12, pp. 5290–5303, Dec. 2016.

[4] F. Muhammad, Z. H. Abbas, and F. Y. Li, "Cell association with load balancing in nonuniform heterogeneous cellular networks: Coverage probability and rate analysis," *IEEE Trans. Veh. Technol.*, vol. 66, no. 6, pp. 5241–5255, Jun. 2017, doi: 10.1109/TVT.2016.2614696.

[5] A. Gupta and R. K. Jha, "A survey of 5G network: Architecture and emerging technologies," *IEEE Access*, vol. 3, pp. 1206–1232, Jul. 2015.

[6] A. Damnjanovic *et al.*, "A survey on 3GPP heterogeneous networks," *IEEE Wireless Commun.*, vol. 18, no. 3, pp. 10–21, Jun. 2011.

[7] Y. Wang and K. Pedersen, "Performance analysis of enhanced inter-cell interference coordination in LTE-advanced heterogeneous networks," in *Proc. IEEE Veh. Technol. Conf. (VTC),* Yokohama, Japan, May 2012, pp. 1–5.

[8] *Aspects of PICO Node Range Extension*, document 3GPP TSG RAN WG1 meeting 61, R1-103824, Nokia Siemens Networks, Nokia, 2010. [Online]. Available: http://goo.gl/XDKXI

[9] V. Chandrasekhar and J. G. Andrews, "Uplink capacity and interference avoidance for two-tier femtocell networks," *IEEE Trans. Wireless Commun.*, vol. 8, no. 7, pp. 3498–3509, Jul. 2009.

[10] P. Lee, T. Lee, J. Jeong, and J. Shin, "Interference management in LTE femtocell systems using fractional frequency reuse," in *Proc. 12th Int. Conf. Adv. Commun. Technol. ICT Green Growth Sustain. Develop. (ICACT)*, vol. 2. Phoenix Park, South Korea, Feb. 2010, pp. 1047–1051,

[11] N. Saquib, E. Hossain, and D. I. Kim, "Fractional frequency reuse for interference management in LTE-advanced hetnets," *IEEE Wireless Commun.*, vol. 20, no. 2, pp. 113–122, Apr. 2013.

[12] P. Jacob, A. James, and A. S. Madhukumar, "Downlink interference reduction through reverse frequency allocation," in *Proc. Int. Conf. Commun. Syst. (ICCS)*, Singapore, Nov. 2012, pp. 329–333.

[13] D. Lépez-Pérez, I. Guvenc, G. de la Roche, M. Kountouris, T. Q. S. Quek, and J. Zhang, "Enhanced intercell interference coordination challenges in heterogeneous networks," *IEEE Wireless Commun.*, vol. 18, no. 3, pp. 22–30, Jun. 2011.

[14] Y. Dhungana and C. Tellambura, "Multi-channel analysis of cell range expansion and resource partitioning in two-tier heterogeneous cellular networks," *IEEE Trans. Wireless Commun.*, vol. 15, no. 3, pp. 2394–2406, Mar. 2016.

[15] M. Čierny, H. Wang, R. Wichman, Z. Ding, and C. Wijting, "On number of almost blank sub-frames in heterogeneous cellular networks," *IEEE Trans. Wireless Commun.*, vol. 12, no. 10, pp. 5061–5073, Oct. 2013.

[16] S. Singh and J. G. Andrews, "Joint resource partitioning and offloading in heterogeneous cellular networks," *IEEE Trans. Wireless Commun.*, vol. 13, no. 2, pp. 888–901, Feb. 2014.

[17] *Further Advancements for E-UTRA Physical Layer Aspects (Release 9)*, document TR 36.814, 3GPP, Mar. 2010.

[18] A. J. Goldsmith, *Wireless Communications*. Cambridge, U.K.: Cambridge Univ. Press, 2005.

[19] S. N. Chiu, D. Stoyan, W. S. Kendall, and J. Mecke, *Stochastic Geometry and Its Applications*, 3rd ed. Hoboken, NJ, USA: Wiley, 2013.

[20] F. Baccelli and B. Blaszczyszyn, "Stochastic geometry and wireless networks," in *Foundations and Tends in Networking*, vol. 1. Breda, The Netherlands: NoW Publishers, 2009.

[21] H.-S. Jo, Y. J. Sang, P. Xia, and J. G. Andrews, "Heterogeneous cellular networks with flexible cell association: A comprehensive downlink SINR analysis," *IEEE Trans. Wireless Commun.*, vol. 11, no. 10, pp. 3484–3495, Oct. 2012.

[22] H. S. Dhillon, R. K. Ganti, F. Baccelli, and J. G. Andrews, "Modeling and analysis of K-tier downlink heterogeneous cellular networks," *IEEE J. Sel. Areas Commun.*, vol. 30, no. 3, pp. 550–560, Apr. 2012.

[23] J. G. Andrews, F. Baccelli, and R. K. Ganti, "A tractable approach to coverage and rate in cellular networks," *IEEE Trans. Commun.*, vol. 59, no. 11, pp. 3122–3134, Nov. 2011.

[24] D. Lépez-Pérez, A. Valcarce, G. de la Roche, and J. Zhang, "OFDMA femtocells: A roadmap on interference avoidance," *IEEE Commun. Mag.*, vol. 47, no. 9, pp. 41–48, Sep. 2009.

[25] H. Wang, X. Zhou, and M. C. Reed, "Analytical evaluation of coverage oriented femtocell network deployment," in *Proc. IEEE Int. Conf. Commun.*, Budapest, Hungary, Jun. 2013, pp. 5974–5979.

[26] J. S. Ferenc and Z. Néda, "On the size distribution of Poisson Voronoi cells," *Phys. A, Statist. Mech. Appl.*, vol. 385, no. 2, pp. S18–S26, Nov. 2007.

[27] S. Singh, F. Baccelli, and J. G. Andrews, "On association cells in random heterogeneous networks," *IEEE Wireless Commun. Lett.*, vol. 3, no. 1, pp. 70–73, Feb. 2014.

[28] S. Singh, H. S. Dhillon, and J. G. Andrews, "Offloading in heterogeneous networks: Modeling, analysis, and design insights," *IEEE Trans. Wireless Commun.*, vol. 12, no. 5, pp. 2484–2497, May 2013.

[29] M. Haenggi. (May 2013). "A versatile dependent model for heterogeneous cellular networks." [Online]. Available: https://arxiv.org/abs/1305.0947

ZIAUL HAQ ABBAS received the M.Phil. degree in electronics from Quaid-e-Azam University, Pakistan, in 2001, and the Ph.D. degree with the Agder Mobility Lab, Department of Information and Communication Technology, University of Agder, Norway, in 2012. He joined the GIK Institute of Engineering Sciences and Technology, Pakistan, as a Research Associate. In 2012, he was a Visiting Researcher with the Department of Electrical and Computer Engineering, University of Minnesota, USA, and joined the Ghulam Ishaq Khan Institute of Engineering Sciences and Technology, Pakistan, where he is currently serving as an Assistant Professor. His research interests include energy efficiency in hybrid mobile and wireless communication networks, 4G and beyond mobile systems, mesh and ad hoc networks, traffic engineering in wireless networks, performance evaluation of communication protocols and networks by analysis and simulation, quality-of-service in wireless networks, green wireless communication, and cognitive radio.

FAZAL MUHAMMAD received the B.Sc. and M.S. degrees in electrical engineering from the University of Engineering and Technology, Peshawar, Pakistan, in 2004 and 2007, respectively, and the Ph.D. degree from the Ghulam Ishaq Khan Institute of Engineering Science and Technology, Topi, Pakistan, in 2017. In 2017, he joined the City University of Science and Information Technology, Peshawar, as an Assistant Professor. His research is focused on the modeling and analysis of heterogeneous cellular networks using tools from stochastic geometry, point process theory, and spatial statistics. His other research interests include interference channels, cognitive radio networks, and mmWave.

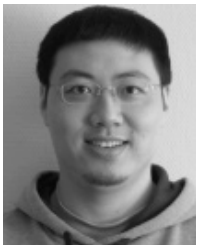

LEI JIAO received the B.E. degree in telecommunication engineering from Hunan University, in 2005, the M.E. degree in communication and information system from Shandong University, China, in 2008, and the Ph.D. degree in information and communication technology from the University of Agder (UiA), Norway, in 2012. He is currently with the Department of Information and Communication Technology, University of Agder, as an Associate Professor. His research interests include mobile communications and artificial intelligence.